**Yadav, S.; Koenen, M.; Bale, N.; Sinninghe Damsté, J.S.; Villanueva, L.** (2021). The physiology and metabolic properties of a novel, low-abundance *Psychrilyobacter* species isolated from the anoxic Black Sea shed light on its ecological role. *Environmental Microbiology Reports 13(6)*: 899-910. DOI: 10.1111/1758-2229.13012

Published version: https://dx.doi.org/10.1111/1758-2229.13012

NIOZ Repository: http://imis.nioz.nl/imis.php?module=ref&refid=347038

[Article begins on next page]

# The physiology and metabolic properties of a novel, low-abundance *Psychrilyobacter* species isolated from the anoxic Black Sea shed light on its ecological role

**Running title**: Physiology of a novel *Psychrilyobacter* sp.

**Keywords**: *Fusobacteria*; *Psychrilyobacter*; Black Sea; Piezotolerance; Energy metabolism

Subhash Yadav[1], Michel Koenen[1], Nicole Bale[1],

Jaap S. Sinninghe Damsté[1,2], and Laura Villanueva[1,2]

[1]NIOZ Royal Netherlands Institute for Sea Research, Department of Marine Microbiology and Biogeochemistry, P.O. Box 59, 1797AB Den Burg, Texel, The Netherlands.

[2]Faculty of Geosciences. Department of Earth Sciences, Utrecht University., P.O. Box 80.021, 3508 TA Utrecht, The Netherlands.

*****Correspondence: Subhash Yadav, NIOZ Royal Netherlands Institute for Sea Research, Department of Marine Microbiology and Biogeochemistry, P.O. Box 59, 1797AB Den Burg, Texel, The Netherlands. Phone No. +31 222 369 427

E-mail: subhash.yadav@nioz.nl

**Summary**

Members of the *Psychrilyobacter* spp. of the phylum *Fusobacteria* have been recently suggested to be amongst the most significant primary degraders of the detrital organic matter in sulfidic marine habitats, despite representing only a small proportion (<0.1%) of the microbial community. In this study, we have isolated a previously uncultured *Psychrilyobacter* species (strains $SD5^T$ and BL5; *Psychrilyobacter piezotolerans* sp. nov.) from the sulfidic waters (i.e., 2,000 m depth) of the Black Sea and investigated its physiology and genomic capability in order to better understand potential ecological adaptation strategies. *P. piezotolerans* utilized a broad range of organic substituents (carbohydrates and proteins) and, remarkably, grew at sulfide concentrations up to 32 mM. These flexible physiological properties were supported by the presence of the respective metabolic pathways in the genomes of both strains. Growth at varying hydrostatic pressure (0.1-50 MPa) was sustained by modifying its membrane lipid composition. Thus, we have isolated a novel member of the "rare biosphere", which endures the extreme conditions and may play a significant role in the degradation of detrital organic matter sinking into the sulfidic waters of the Black Sea.

## Introduction

The existence of the "rare biosphere" (Sogin *et al*., 2006) still remains an incompletely understood phenomenon in microbial ecology, partly due to the limited knowledge of the physiology of the microbes present in low abundance. As an example, free-living *Psychrilyobacter* spp. of the phylum *Fusobacteria* have been recently reported to be present in extremely low abundance (i.e., representing <0.1% of the microbial community) in subarctic marine sediments but have been proven to be amongst the most important degraders (i.e., 10 % of the total) of the protein component of the detrital organic matter of this system (Müller *et al*., 2018; Pelikan *et al*., 2020), and also in anoxic tidal flat sediments (Graue *et al*., 2012). *Psychrilyobacter* spp. 16S rRNA gene sequences have also reported to be under detection level in the subsurface waters of the Gulf of Mexico but became abundant (~40%) after the Deepwater Horizon oil spill, probably due to the potential capacity of the members of this genus for hydrocarbon degradation under anoxic conditions (Gutierrez *et al*., 2016). Some of these studies applied methods beyond 16S rRNA gene amplicon sequencing e.g., ecophysiological analyses based on stable-isotope probing and metagenomics. Nevertheless, little is known about the physiology and adaptation strategies of these members of the *Fusobacteria* phylum as part of the "rare biosphere" in marine habitats".

In this study, we have examined the distribution and abundance of fusobacterial members in the Black Sea water column. The Black Sea is the largest permanent anoxic basin on Earth, with a maximum depth of approximately 2,200 meters. The Black Sea deep waters (> 2,000 m) are characterized recalcitrant nutrient conditions (i.e., the presence of difficult to degrade sulfurized dissolved organic matters; Gomez-Saez *et al*.,

2021), elevated hydrostatic pressure and high sulfide concentration (400 µM; Volkov and Neretin, 2007), conditions which are expected to harbor microorganisms adapted to deal with those conditions (e.g., Vetriani *et al*., 2003; Wakeham *et al*., 2003; Lin *et al*., 2006; Leloup *et al*., 2007; Wakeham *et al*., 2007; Henkel *et al*., 2019; Suominen *et al*., 2021a; Suominen *et al*., 2021b; Yadav *et al*., 2020). Here, we have successfully enriched members of the genus *Psychrilyobacter* (up to 58% of the total microbial community) of the phylum *Fusobacteria* and isolated two representative strains (*Psychrilyobacter* sp. strains SD5$^{T}$ and BL5) from the deep sulfidic waters of the Black Sea (i.e., 2,000 m depth). To elucidate their role in the sulfidic waters of the Black Sea, we investigated the genome sequences of the isolated strains, and tested their physiology and adaptation strategies by mimicking the *in situ* physicochemical conditions (i.e., elevated hydrostatic pressure, high sulfide concentration). Our study demonstrates the successful enrichment and isolation of a novel member (*Psychrilyobacter piezotolerans*) of the "rare biosphere" and sheds light onto its potential ecological relevance in sulfidic marine habitats.

## Results and Discussion

### Distribution and ecology of *Fusobacteria* in the Black Sea water column

Overall, 16S rRNA gene amplicon sequencing analysis revealed that *Fusobacteria*-affiliated sequences were present in low abundance in the Black Sea water column, representing <0.01% of all 16S rRNA gene sequences identified throughout the water column (Fig. 1C). Estimated fusobacterial 16S rRNA gene copy numbers ranged between 0.4-5.0 x $10^{3}$ $L^{-1}$ in the Black Sea water column in the 50- 2,000 m depth range, with the lowest estimated abundances at 50 m (Fig. 1B). The highest estimated abundance of both *Fusobacteria* and *Psychrilyobacter* 16S rRNA gene sequences was

93 detected at 120-150 m depth within the chemocline. This zone could be most favorable
94 for these microorganisms due to the suboxic-anoxic conditions, availability of various
95 nutrients [e.g., $NH_4^+$ (~14 µM), $PO_4^{3-}$ (~5.5 µM; Fig. 1A), presence of dissolved organic
96 carbon (~200 µM; Suominen *et al*., 2021b), and relatively low hydrostatic pressure (1.2-
97 1.5 MPa). Phylogenetic analysis, based on the 16S rRNA gene amplicon sequences
98 attributed to *Fusobacteria* recovered from the Black Sea water column, revealed that they
99 represent seven putative clades within this phylum (Fig. 1C). Sequences of most of these
100 operational taxonomic units (OTUs) [(i.e., those falling in clade V ($SD5^T$, BL5 and
101 closely related sequences) and VI (*Leptotrichiaceae*-related sequences)] were distributed
102 throughout the water column (Fig. 1B). However, 16S rRNA gene sequences of a few
103 taxa within the phylum *Fusobacteria*, like *Cetobacterium* (clade III), were only detected
104 at 2,000 m. Sequences affiliated to *Psychrilyobacter*, the most abundant group within
105 *Fusobacteria* (i.e., representing 60-100% of all fusobacterial 16S rRNA gene sequences;
106 Fig. 1B), were encountered in waters ranging from 50 to 2,000 m. The presence of the
107 *Psychrilyobacter* 16S rRNA gene sequences in the oxic zone (50 m; $O_2$ concentration
108 121 µM) is intriguing, since members of the phylum *Fusobacteria* have been described to
109 be strict anaerobes (Janssen and Liesack, 1995; Brune *et al*., 2002; Hofstad, 2006; Zhao
110 *et al*., 2009).

111 **Enrichment and isolation of *Psychrilyobacter* spp.**

112 The 16S rRNA gene composition of enrichments grown in media BS1, BS2 and
113 BS3 (containing cellulose and tryptone as nutrient sources) revealed that sequences
114 affiliated to the *Psychrilyobacter* genus represented 32-58% of the total microbial
115 community (Supplementary Fig. 1) with a high density of rod to oval shaped cells (Fig.

2). Repeated streaking resulted in the isolation of two bacterial strains, designated SD5$^T$ (type strain, T, characterized based on a polyphasic taxonomic approach) and BL5. As *Psychrilyobacter* 16S rRNA gene sequences had been detected in the oxic and suboxic zones of the Black Sea (Fig. 1B), the isolated strains were tested for growth under aerobic and microaerophilic conditions but turned out to be strict anaerobes. Both strains were non-spore forming bacteria and showed negative reaction for oxidase and catalase activities, in agreement with their anaerobic lifestyle. Their 16S rRNA gene sequences were identical and they shared 100% similarity with 16S rRNA gene amplicon sequences of *Psychrilyobacter* (considering the ca. 300 bp fragment used for the 16S rRNA gene amplicon analysis) obtained from various depth of the Black Sea waters (Fig. 1).

**General genomic features and phylogenetic affiliation of strains SD5$^T$ and BL5**

Whole genome sequencing of the strains SD5$^T$ and BL5 yielded genomes of 3,358,809 bp and 3,344,081 bp in length, respectively, which were almost complete (98.88%) and free of contamination (Supplementary Table S1). The G+C mol% of the SD5$^T$ and BL5 was 33.85% and 33.83%, respectively. No CRISPR repeats, signatures of viral infection (Sorek *et al*., 2008), were identified. Viral lysis of bacteria depends on the encounter possibilities, which are fewer for low abundant microbial taxa (Wilcox and Fuhrman, 1994). Hence, the absence of CRISPR repeats indicates that *Psychrilyobacter* spp. are probably not affected by viral predation due to their extremely low abundance in the Black Sea water column.

The phylogenomic analysis based on the concatenation of 49 marker genes (Fig. 3; see supplementary information for methods) showed that both strains clustered with *Psychrilyobacter atlanticus* DSM 19335$^T$. In addition, they showed 99.5% 16S

rRNA gene sequence similarity with *Psychrilyobacter atlanticus* DSM 19335$^T$. However, average nucleotide identity (ANI) and digital DNA-DNA hybridization (DDH) between *Psychrilyobacter atlanticus* DSM 19335$^T$ and strains SD5$^T$ and BL5 were only 86.6% and 32.9%, respectively (Supplementary Table S3), suggesting that both strains belong to a novel species in the genus *Psychrilyobacter* of the phylum *Fusobacteria*.

Members of the phylum *Fusobacteria* are adapted to two contrasting lifestyles i.e., free-living and host associated. Our genome-based phylogeny separates these two types to some extent (Fig. 3): strains SD5$^T$ and BL5, which are adapted to a free-living lifestyle, are more closely related to other fusobacteria with a free-living lifestyle. However, previous 16S rRNA gene-based studies indicated that their closest phylogenetic neighbors are associated with various marine organisms that do possess a host-associated lifestyle (Li *et al*., 2012; Bik *et al*., 2016; Lai *et al*., 2020; Nelson *et al*., 2013; Fernandez-Piquer *et al*., 2012; Palmer *et al*., 1994; Eisenberg *et al*., 2016; Aronson *et al*., 2017; Friel *et al*., 2020). For example, *Psychrilyobacter* spp. are reported as the most abundant bacteria in pacific oysters and gut of the Antarctic seals (Nelson *et al*., 2013; Fernandez-Piquer *et al*., 2012). Indeed, the size of the genomes of strains SD5$^T$ and BL5 is larger (ca. 3.35 Mb; Supplementary Table S1) than that of their host-associated phylogenetic neighbors (ca. 2.3 Mb). They also possessed relatively higher genomic G+C content, a greater gene repertoire and a higher number of tRNAs (Supplementary Table S1). Such genomic properties are often possessed by free-living bacteria in comparison to their host-associated stages (Moran and Plague, 2004; Moran and Wernegreen, 2000; Moya *et al*., 2008; Merhej *et al*., 2009; Klasson and Andersson, 2004; Wernegreen, 2005) supporting their free-living lifestyle. Moreover, it is still possible to observe genomic

traits of their potential host-associated ancestor, such as putative virulence factors (Supplementary Fig. 2) and the isoprenoid MEP/DOXP pathway, which has been previously related to pathogenicity (Sarowska *et al*., 2019) and intracellular survival (Shin *et al*., 2006; Begley *et al*., 2004), respectively. Hence, we assume that these strains also have the potential to colonize higher organisms in a host-associated lifestyle.

**Physiology**

Strains SD5$^{T}$ and BL5 hydrolyzed complex polysaccharides such as cellulose, chitin, salicin and starch, and grew anaerobically by fermenting a wide range of various carbon sources (Supplementary Table S4). Among all carbon sources tested for growth, pyruvate was utilized preferably by both strains (Supplementary Table S4). They hydrolyzed proteins and grew well by fermenting various amino acids, i.e., threonine, lysine, glutamate, and aspartate (Supplementary Table S4). The range of compounds that can support growth of the novel isolates is very broad which includes various organic substituents derived from biogenic remains (Supplementary Table S4). Their growth was also improved by acetate which indicates its utilization as carbon and energy source. Considering both the physiology and genomic signatures, it is likely that their capacity to hydrolyze and ferment a wide range of carbohydrates and amino acids allows them to use the detrital organic matter sinking through the sulfidic waters (Diercks and Asper, 1997). This is supported by their high abundance in the nutrient-rich medium mimicking the *in-situ* physicochemical conditions (Supplementary Fig. 2). Our results further support that *Psychrilyobacter* spp. could be important detrital organic matter degraders along with other anaerobic bacteria in sulfidic marine sediments (Graue *et al*., 2012; Müller *et al*., 2018; Pelikan *et al*., 2020).

We tested our strains for growth at sulfide concentration ranging from 0.1-40 mM. Interestingly, both strains were able to grow at sulfide concentrations up to 32 mM at pH 7.0, which is 80-fold the natural concentration found in the Black Sea deep waters (i.e., 400 μM). To the best of our knowledge, growth at such high sulfide concentration has not been reported for any organisms. At lower (<4 mM) sulfide concentration, the cells appeared as chains of rods (0.6-0.7 x 4.0-6.0 μm), but at higher (>4 mM) sulfide concentration few cells appeared spherical with 0.8-0.9 μm in diameter (Figs. 2A-D). They also showed the presence of sulfur granules in the cell (e.g., Fig. 2C). At 32 mM sulfide concentration, both strains grew in chains of brightly shining cells because of the presence of refractive sulfur granules (Fig. 2E). Growth of both strains was relatively slower in the presence of higher (>7 mM) sulfide concentration and the doubling time extended from 2-3 h at optimal conditions to up to 5-7 h (Fig. 4A).

Strains SD5$^{T}$ and BL5 were able to grow up to 50 MPa of hydrostatic pressure under strict anaerobic conditions. However, growth slowed down at elevated hydrostatic pressure (>20 MPa). Addition of glutamate (0.01%) to the growth medium slightly increased growth at elevated hydrostatic pressure (30 MPa; Fig. 4). This is expected since glutamate functions as one of the most prominent compatible solutes under stress conditions (Csonka, 1989). Glutamate has been previously reported as a “piezolite” in *Desulfovibrio hydrothermalis*, where it significantly improved the growth at elevated hydrostatic pressure (Amrani *et al*., 2014). In addition, glutamate allows enzymes to function efficiently (Brown, 1990; Walker and van der Donk, 2016), eventually protecting macromolecular structures to maintain metabolic functions at elevated hydrostatic pressure (Welsh, 2000; Bhaganna *et al*., 2010).

We also investigated the effect of elevated hydrostatic pressure on the composition of the cell membrane core lipid (CL) and intact polar lipid (IPL) composition of strain SD5$^{T}$. Overall, the core lipid distribution was similar between the strains grown at 0.1 and 20 MPa but changed significantly for the strain grown at 30 MPa. In the cultures grown at 0.1 and 20 MPa, the relative abundance of unsaturated fatty acids (not including hydroxy fatty acids) was 30 and 35%, respectively (Table 1), while at 30 MPa this had increased to 56%. Similarly, earlier studies have also reported a prominent correlation between growth at elevated hydrostatic pressure and increase of the unsaturated fatty acid content (Yadav *et al*., 2020, Allen *et al*., 1999; Grossi *et al*., 2010). Another observed change in the core lipid distribution was that the abundance of hydroxy fatty acids, probably derived from Lipid A in the lipopolysaccharides (LPS) layer; it decreased with increasing pressure (Table 1). The total hydroxy fatty acids decreased from 18 to 14 to 10% as growth pressure increased from 0.1 to 20 to 30 MPa. Likewise, a decrease in the relative abundance of hydroxy fatty acids has been observed in *Profundimonas piezophila* grown at elevated hydrostatic pressure (Cao *et al*., 2014). Alterations in the relative abundance of hydroxy fatty acids are expected to change cell membrane properties by affecting the polarity of core lipids (Nichols *et al*., 2004). However, there are no detailed studies available related with the physical role of hydroxy fatty acids in the adaptation of cellular membranes under elevated hydrostatic pressure. An increase in hydroxy fatty acids has been observed in psychrophilic bacteria upon cold adaptation (Bale *et al*., 2019). Consequently, it could be hypothesized that a decrease in the relative abundance of hydroxy acids could be induce by elevated hydrostatic pressure, while an increase in the membrane unsaturated fatty acids is an adaptation to conditions

231 in the strains under study here. This change agrees with the fact that polyunsaturated fatty
232 acids chain implement a more expanded conformation with lower melting temperatures
233 than their saturated counterparts allowing the cell membrane flexibility at higher
234 hydrostatic pressure (Hazel *et al*., 1990).

235 A notable change of the IPL head group composition with increasing pressure was
236 observed between 20 MPa and 30 MPa (Table 2). Of the IPL headgroups, the largest
237 change was in the relative abundance of phosphatidylglycerol (PG), which was 19 and
238 24% at 0.1 and 20 MPa, respectively but 51% at 30 MPa (Table 2). The largest
239 concomitant decrease was in the cardiolipins (including lyso-cardiolipins): from 38 and
240 45% at 0.1 and 20 MPa, respectively, to 22% at 30 MPa (Table 2). This shift may be an
241 adaptive process relating to membrane fluidity at elevated hydrostatic pressure. To date,
242 there are no other reports of such specific membrane adaption under high hydrostatic
243 pressure in piezophilic bacteria. The nitrogen-containing headgroup PC also decreased in
244 relative abundance (Supplementary Table 2) with increasing pressure (17.8, 6.0 and 7.6
245 % at 0.1, 20 and 30 MPa, respectively). An increase in PG relative to PE with increasing
246 pressure has been previously observed in the piezo-sensitive bacterium, *Vibrio* sp. strain
247 LT25 (Mangelsdorf *et al*., 2005) and in *Desulfovibrio indonesiensis* strain P23 at certain
248 temperatures (Fichtel *et al*., 2015). Conversely, PG was reported to decrease relative to
249 PE with increasing pressure, for the piezophilic bacterial strains 16C1 and 2D2 (Yano *et*
250 *al*., 1998).

251 **Metabolism based on genomic analysis**

252 Genomes of both strains contained genes related to aerotolerance (i.e., superoxide
253 reductase, ruberythrin and thioredoxin reductase; Fig. 5), which might be an adaptation to

survive in oxic and suboxic zone of the Black Sea. They utilized a wide range of carbon and nitrogen sources which is supported by the presence of various genes in the genomes (Fig. 5; Supplementary Table S2). Genes encoding enzymes involved in glucose fermentation, i.e., production of acetate, ethanol, lactate, formate, hydrogen and carbon dioxide (Fig. 5; Supplementary Table S2), and acetate utilization were identified. The presence of seven putative [FeFe]-hydrogenase genes involved in the generation of $H_2$ during carbohydrate and protein fermentations in various microorganisms were also annotated (Greening *et al*., 2016; Wolf *et al*., 2016). This is further supported by the presence of pyruvate-formate lyase and pyruvate-ferredoxin oxidoreductase genes in the genomes (Fig. 5; Supplementary Table S2).

The two known genes for sulfide oxidation i.e., sulfide-quinone-oxidoreductase (*sqr*) and flavocytochrome *c* sulfide dehydrogenase were not detected in the genomes. However, sulfide oxidation may be catalyzed by some unclassified flavoproteins encoded by the genomes. We could detect seven gene copies coding for rhodanese (EC 2.8.1.1; Fig. 6; Supplementary Table S2), which are involved in sulfur trafficking and oxidation in bacteria (Dahl, 2017; Koch and Dahl, 2018). Rhodanese cleaves the S-S bond present in thiosulfate, producing sulfur and sulfite (Dahl, 2017; Koch and Dahl, 2018). A complete set of genes encoding the enzymes involved in the heterodisulfide reductase (HDR) system (Fig. 5; Supplementary Table S2), acting as an elemental sulfur oxidation enzyme in the cytoplasmic space of bacteria and archaea (Wang *et al*., 2019), was also identified. Their presence suggests the involvement in sulfur metabolism and potentially in the alleviation of sulfidic toxicity in the *Psychrilyobacter* spp. at elevated sulfide concentrations.

We also observed the presence of the genes encoding enzymes in the glutamine synthetase (GS) and glutamate synthase (GOGAT) pathway, and glutamate and glutamine transporters in the genomes of the strains SD5$^{T}$ and BL5 (Fig. 5; Supplementary Table S2). These genes have been reported to aid in the osmoregulation and survival mechanisms in piezophilic bacteria (Csonka, 1989; Kang and Hwang, 2018). Therefore, the GS/GOGAT pathway and glutamate transporters (Fig. 5) might be involved in the cell internalization of extracellular glutamate and other solutes in *Psychrilyobacter* strains to survive at elevated hydrostatic pressures in the deep sulfidic waters of the Black Sea.

All genes involved in 2-*C*-methyl-D-erythritol 4-phosphate/1-deoxy-D-xylulose 5-phosphate (MEP/DOXP) pathway of isoprenoid biosynthesis were identified in the genomes of the strains SD5$^{T}$ and BL5 (Fig. 5; Supplementary Table S1-S2). We could only detect the phosphomevalonate decarboxylase coding gene of the mevalonate pathway for isoprenoid biosynthesis. Nevertheless, growth of both strains in the medium amended with either/both fosmidomycin [a pathway inhibitor of 2-*C*-methyl-D-erythritol 4-phosphate (MEP) pathway] and simvastatin (a pathway inhibitor of mevalonate pathway) suggested that both MEP and mevalonate isoprenoid biosynthetic pathways were functional. Hence, the evidence for the presence and potential functionality of both isoprenoid biosynthetic pathways in these strains is enigmatic and requires further study to validate their role.

**Conclusions**

*Psychrilyobacter* spp. typically belong to the “rare biosphere” in marine environments but incubation studies have identified them to be major degraders of

organic matter in sulfidic marine sediments. Here, we isolated two representative strains of *Psychrilyobacter,* which are adapted to both elevated hydrostatic pressure and the high sulfide concentrations of the Black Sea deep water column. Their ability to use a variety of organic substituents and adaptations to various environmental stressors help them to endure with the conditions of the Black Sea. This demonstrates the versatile metabolic potential of a member of the "rare biosphere", which harbors adaptable strategies to deal with various environmental stressors. However, despite these versatile traits, *Psychrilyobacter* spp. remains a quantitatively minor member of the microbial community of the Black Sea for unknown reasons. Incubation studies may therefore provide a quantitatively unrealistic view of the microbes involved in anaerobic organic matter degradation. Overall, our study evidently suggests that a collective approach i.e., the stimulations by organic rich substances, enrichments and isolation in conjunction with culture-independent methods, are required to unravel the ecological relevance of free-living *Fusobacteria* in sulfidic marine habitats.

**Description of *Psychrilyobacter piezotolerans* sp. nov.**

*Psychrilyobacter piezotolerans* (pie.zo.to′le.rans. Gr. v. *piezo* to press; L. part. adj. *tolerans* tolerating, N.L. part. adj. *piezotolerans* tolerating high hydrostatic pressure).

**Properties**: Cells are motile and rod (0.6-0.7 x 3-6 μm) shaped. Cell shape change from rod to spherical shape (diameter, 1.1-1.2) under higher sulfide concentration (>4 mM). Cells stain Gram-negative and are obligate anaerobes. Growth occurs between pH 6.5-8.8 (optimum 7.0-8.0). Tolerates up to 5.5% NaCl with optimum growth at 2-3%. Optimum growth occurs at 20-25°C (range 4-35 °C). Glutamate supports the growth at higher hydrostatic pressure. Pyruvate is preferred carbon source for the growth. Yeast extract is

required for growth. Dominant fatty acids (>10%) are: $C_{16:0,}$ $C_{16:1}$ ω9C and $C_{14:0}$. Fatty acids in moderate abundance (4-10%) are: *β*-OH $C_{12:0}$ and *β*-OH $C_{16:0}$. Phosphatidylethanolamine (PE), phosphatidylglycerol (PG), cardiolipins and lyso-PE are major polar lipids. G+C content is 33.8%. Type strain is $SD5^T$ (JCM $32482^T$= KCTC $15663^T$).

## Author Contributions

SY, LV and JSSD designed the study. SY performed most of the laboratory work and data analysis; MK and NB performed the fatty acid and intact polar lipid analysis; SY, LV and JSSD wrote the manuscript.


## Funding Information

This research was supported by the SIAM Gravitation Grant (024.002.002) from the Dutch Ministry of Education, Culture and Science (OCW) to JSSD and LV. JSSD and NB received funding from the European Research Council (ERC) under the European Union's Horizon 2020 research and innovation program (Grant Agreement No. 694569) funded to JSSD.


## Conflict of interest statement

The authors declare that there are no conflicts of interest.


## Acknowledgements

The authors are thankful to Marianne Baas for helping in fermentation product (gas phase) analysis, to Sanne Vreugdenhil and Maartje Brouwer for their support with the molecular genetic analyses, and to Denise Dorhout for lipid analysis. We would like to thank the cruise leader, captain, crew, and scientific participants of Black Sea

expedition-2017 (64PE418) on board of the *R/V* Pelagia for sampling and technical support.

**References**

Allen, E.E., Facciotti, D., and Bartlett, D.H. (1999) Monounsaturated but not polyunsaturated fatty acids are required for growth of the deep-sea bacterium *Photobacterium profundum* SS9 at high pressure and low temperature. *Appl Environ Microbiol* **65**: 1710-1720.

Amrani, A., Bergon, A., Holota, H., Tamburini, C., Garel, M., Ollivier, B., *et al*. (2014). Transcriptomics reveal several gene expression patterns in the piezophile *Desulfovibrio hydrothermalis* in response to hydrostatic pressure. *PLoS ONE* **9**: e106831.

Arkin, A.P., Cottingham, R.W., Henry, C.S., Harris, N.L., Stevens, R.L., Maslov, S., *et al*. (2018) KBase: The United States Department of Energy Systems Biology Knowledgebase. *Nat Biotechnol* **36**: 566.

Aronson, H.S., Zellmer, A.J., and Goffredi, S.K. (2017) The specific and exclusive microbiome of the deep-sea bone-eating snail, *Rubyspira osteovora*. *FEMS Microbiol Ecol* **93**: 10.

Bale, N.J., Sorokin, D.Y., Hopmans, E.C., Koenen, M., Rijpstra, W.I.C., Villanueva, L., *et al.* (2019). New insights into the polar lipid composition of extremely halo(alkali)philic euryarchaea from hypersaline lakes. *Front Microbiol* **10**: 377.

Begley, M., Gahan, C.G., Kollas, A.K., Hintz, M., Hill, C., Jomaa, H., Eberlm, M. (2004) The interplay between classical and alternative isoprenoid biosynthesis controls gammadelta T cell bioactivity of *Listeria monocytogenes*. *FEBS Lett* **12**: 99-104.

Bhaganna, P., Volkers, R.J.M., Bell, A.N.W., Kluge, K., Timson, D.J., McGrath, J.W., *et al*. (2010) Hydrophobic substances induce water stress in microbial cells. *Microb Biotechnol* **3**: 701-716.

Bik, E.M., Costello, E.K., Switzer, A.D., Callahan, B.J., Holmes, S.P., Wells, R.S., *et al.* (2016) Marine mammals harbor unique microbiotas shaped by and yet distinct from the sea. *Nat Commun* **7**: 10516.

Brown, A.D. (1990) Microbial Water Stress Physiology. Principles and Perspectives. Chichester, UK: John Wiley & Sons Ltd.

Brune, A., Evers, S., Kaim, G., Ludwig, W., and Schink, B. (2002) *Ilyobacter insuetus* sp. nov., a fermentative bacterium specialized in the degradation of hydroaromatic compounds. *Int J Syst Evol Microbiol* **52**: 429-432.

Cao, Y., Chastain, R.A., Eloe, E.A., Nogi, Y., Kato, C., and Bartlett, D.H. (2014) Novel psychropiezophilic *Oceanospirillales* species *Profundimonas piezophila* gen. nov., sp. nov., isolated from the deep-sea environment of the Puerto Rico trench. *Appl Environ Microbiol* **80**: 54-60.

Csonka, L.N., (1989) Physiological and genetic responses of bacteria to osmotic stress. *Microbiol Rev* **53**: 121-147.

Dahl, C. (2017). Sulfur metabolism in phototrophic bacteria. In: Hallenbeck P. (eds) Modern Topics in the Phototrophic Prokaryotes. Springer, Cham. https://doi.org/10.1007/978-3-319-51365-2_2.

Diercks, A.R., Asper, V.L. (1997). In situ settling speeds of marine snow aggregates below the mixed layer: Black Sea and Gulf of Mexico. Deep Sea Res. Part I Oceanogr. Res. Pap **44**: 385-398.

Eisenberg, T., Kämpfer, P., Ewers, C., Semmler, T., Glaeser, S.P., Collins, E., *et al*. (2016) *Oceanivirga salmonicida* gen. nov., sp. nov., a member of the *Leptotrichiaceae* isolated from Atlantic salmon (Salmo salar). *Int J Syst Evol Microbiol* **66**: 2429-2437.

Fernandez-Piquer, J., Bowman, J.P., Ross, T., and Tamplin, M.L. (2012) Molecular analysis of the bacterial communities in the live Pacific oyster (*Crassostrea gigas*) and the influence of postharvest temperature on its structure. *J Appl Microbiol* **112**: 1134-43.

Fichtel, K., Logemann, J., Fichtel, J., Rullkötter, J., Cypionka, H., and Engelen, B. (2015) Temperature and pressure adaptation of a sulfate reducer from the deep subsurface. *Front Microbiol* **6**: 1078.

Friel, A.D., Neiswenter, S.A., Seymour, C.O., Bali, L.R., McNamara, G., Leija, F., Jewell, J., and Hedlund, B.P. (2020). Microbiome shifts associated with the introduction of wild Atlantic Horseshoe Crabs (*Limulus polyphemus*) into a touch-tank exhibit. *Front Microbiol* **11**:1398.

Gomez-Saez, G.V., Dittmar, T., Holtappels, M., Pohlabeln, A.M., Lichtschlag, A., Schnetger, B., Boetius, A., and Niggemann, J. (2021). Sulfurization of dissolved organic matter in the anoxic water column of the Black Sea. *Sci Adv* **7**:eabf6199. doi: 10.1126/sciadv.abf6199.

Graue, J., Engelen, B., and Cypionka, H. (2012). Degradation of cyanobacterial biomass in anoxic tidal-flat sediments: a microcosm study of metabolic processes and community changes. *ISME J* **6**:660-669.

413 Greening, C., Biswas, A., Carere, C.R., Jackson, C.J., Taylor, M.C., Stott, M.B., *et al*.
414 (2016). Genomic and metagenomic surveys of hydrogenase distribution indicate
415 $H_2$ is a widely utilised energy source for microbial growth and survival. *ISME J* **10**:
416 761-777.
417 Grossi, V., Yakimov, M.M., Al Ali, B., Tapilatu, Y., Cuny, P., Goutx, M., *et al.* (2010)
418 Hydrostatic pressure affects membrane and storage lipid compositions of the
419 piezotolerant hydrocarbon-degrading *Marinobacter hydrocarbonoclasticus* strain
420 #5. *Environ Microbiol* **12**: 2020-2033.
421 Gutierrez, T., Berry, D., Teske, A., and Aitken, M.D. (2016) Enrichment of *Fusobacteria*
422 in sea surface oil slicks from the Deepwater Horizon oil spill. *Microorganisms* **4**:
423 24.
424 Hazel, J.R., and Williams, E.E. (1990) The role of alterations in membrane lipid
425 composition in enabling physiological adaptation of organisms to their physical
426 environment. *Prog Lipid Res* **29**: 167-227.
427 Henkel, J.V., Dellwig, O., Pollehne, F., Herlemann, D.P.R., Leipe, T., and Schulz-Vogt,
428 H.N. (2019) A bacterial isolate from the Black Sea oxidizes sulfide with manganese
429 (IV) oxide. *Proc Natl Acad Sci USA* **116**: 12153-12155.
430 Hofstad, T. (2006) The Genus *Fusobacterium*. In: Dworkin M., Falkow S., Rosenberg
431 E., Schleifer KH., Stackebrandt E. (eds) The Prokaryotes. Springer, New York,
432 NY.
433 Janssen, P. H., and Liesack, W. (1995) Succinate decarboxylation by *Propionigenium*
434 *maris* sp. nov., a new anaerobic bacterium from an estuarine sediment. *Arch*
435 *Microbiol* **164**: 29-35.

436 Kang, Y., and Hwang, I. (2018) Glutamate uptake is important for osmoregulation and
437 survival in the rice pathogen *Burkholderia glumae*. *PLoS ONE* **13**: e0190431.
438 Klasson, L., and Andersson, S.G.E. (2004) Evolution of minimal-gene-sets in host-
439 dependent bacteria. *Trends Microbiol* **12**: 37-43.
440 Koch, T., and Dahl, C. (2018) A novel bacterial sulfur oxidation pathway provides a new
441 link between the cycles of organic and inorganic sulfur compounds. *ISME J* **12**:
442 2479-2491.
443 Lai, K.P., Lin, X., Tam, N., Ho, J.C.H., Wong, M.K-S., Gu, J., *et al*. (2020) Osmotic
444 stress induces gut microbiota community shift in fish. *Environ Microbiol* **22**: 3784-
445 3802.
446 Leloup, J., Loy, A., Knab, N.J., Borowski, C., Wagner, M., and Jørgensen, B.B. (2007)
447 Diversity and abundance of sulfate-reducing microorganisms in the sulfate and
448 methane zones of a marine sediment, Black Sea. *Environ Microbiol* **9**: 131-142.
449 Lin, X., Wakeham, S.G., Putnam, I.F., Astor, Y.M., Scranton, M.I., Chistoserdov, A.Y.,
450 and Taylor, G.T. (2006) Vertical distributions of prokaryotic assemblages in the
451 anoxic Cariaco Basin and Black Sea compared using fluorescence *in situ*
452 hybridization (FISH) techniques. *Appl Environ Microbiol* **72**: 2679-2690.
453 Mangelsdorf, K., Zink, K.G., Birrien, J.L., and Toffin, L. (2005) A quantitative
454 assessment of pressure dependent adaptive changes in the membrane lipids of
455 piezosensitive deep sub-seafloor bacterium. *Org Geochem* **36**: 1459-1479.
456 Merhej, V., Royer-Carenzi, M., Pontarotti, P., and Raoult, D. (2009) Massive
457 comparative genomic analysis reveals convergent evolution of specialized
458 bacteria. *Biol Direct* **4**: 13.

459 Moran, N.A., and Plaque, G.R. (2004) Genomic changes following host restriction in
460 bacteria. *Curr Opin Genet Dev* **14**: 627-633.
461 Moran, N.A., and Wernegreen, J.J. (2000) Lifestyle evolution in symbiotic bacteria:
462 insights from genomics. *Trends Ecol Evol* **15**: 321-326.
463 Moya, A., Peretó, J., Gil. R., and Latorre, A. (2008) Learning how to live together:
464 genomic insights into prokaryote-animal symbioses. *Nat Rev Genet* **9**: 218-229.
465 Müller, A.L., Pelikan, C., de Rezende, J.R., Wasmund, K., Putz, M., Glombitza, C.,
466 Kjeldsen, K.U., Jørgensen, B.B., and Loy, A. (2018). Bacterial interactions during
467 sequential degradation of cyanobacterial necromass in a sulfidic arctic marine
468 sediment. *Environ Microbiol* **20**: 2927-2940.
469 Nelson, T.M., Rogers, T.L., Carlini, A.R., and Brown, M.V. (2013). The gut microbiota
470 of wild and captive Antarctic seals. *Environ Microbiol* **15**: 1132-1145.
471 Nichols, D.S., Miller, M.R., Davies, N.W., Goodchild, A., Raftery, M., and Cavicchioli,
472 R. (2004) Cold adaptation in the Antarctic Archaeon *Methanococcoides burtonii*
473 involves membrane lipid unsaturation. *J. Bacteriol* **186**: 8508-8515.
474 Palmer, R., Drinan E., and Murphy, T. (1994) A previously unknown disease of farmed
475 Atlantic salmon: pathology and establishment of bacterial aetiology. *Dis Aquat* Org
476 **19**: 7-14.
477 Pelikan, C., Wasmund, K., Glombitza, C., Hausmann, B., Herbold, C.W., Flieder, M.,
478 and Loy, A. (2021). Anaerobic bacterial degradation of protein and lipid
479 macromolecules in subarctic marine sediment. *ISME J* **15**: 833-847**.**
480 Sarowska, J., Futoma-Koloch, B., Jama-Kmiecik, A., Frej-Madrzak, M., Ksiazczyk, M.,
481 Bugla-Ploskonska, G., and Choroszy-Krol, I. (2019) Virulence factors, prevalence,

and potential transmission of extraintestinal pathogenic *Escherichia coli* isolated from different sources: recent reports. *Gut Pathog* **11**: 10.

Shin, S.J., Wu, C.W., Steinberg, H., and Talaat, A.M. (2006) Identification of novel virulence determinants in Mycobacterium paratuberculosis by screening a library of insertional mutants. *Infect Immun* **74**: 3825-3833.

Sogin, M.L., Morrison, H.G., Huber, J.A., Mark, Welch, D., Huse, S.M., Neal, P.R., Arrieta, J.M., and Herndl, G.J. (2006). Microbial diversity in the deep sea and the underexplored "rare biosphere". *Proc Natl Acad Sci USA* **103**: 12115-12120.

Sollai, M., Villanueva, L., Hopmans, E.C., Reichart, G.J., and Sinninghe Damsté J.S. (2019) A combined lipidomic and 16S rRNA gene amplicon sequencing approach reveals archaeal sources of intact polar lipids in the stratified Black Sea water column. *Geobiol* **17**: 91-109.

Sorek, R., Kunin, V., and Hugenholtz, P. (2008) CRISPR a widespread system that provides acquired resistance against phages in bacteria and archaea. *Nat Rev Microbiol* **6**: 181-186.

Suominen, S., Dombrowski, N., Sinninghe Damsté, J.S., and Villanueva, L. (2021a) A diverse uncultivated microbial community is responsible for organic matter degradation in the Black Sea sulfidic zone. *Environ Microbiol* **23**: 2709-2728.

Suominen, S., Doorenspleet, K., Sinninghe Damsté, J.S., and Villanueva, L. (2021b) Microbial community development on model particles in the deep sulfidic waters of the Black Sea. *Environ Microbiol* **23**: 2729-2746.

503 Vetriani, C., Tran, H.V., and Kerkhof, L.J. (2003) Fingerprinting microbial assemblages
504 from the oxic/anoxic chemocline of the Black Sea. *Appl Environ Microbiol* **69**:
505 6481-6488.
506 Villanueva, L., von Meijenfeldt, F. A. B., Westbye, A.B., Yadav, S., Hopmans, E.,
507 Dutilh, B., and Damste, J.S.S. (2021) Bridging the membrane lipid divide: bacteria
508 of the FCB group superphylum have the potential to synthesize archaeal ether
509 lipids. *ISME J* **15**: 168-182.
510 Volkov, I.I., and Neretin, L.N. (2007) Hydrogen sulfide in the Black Sea. The Black Sea
511 Environment. pp 309-331.
512 Wakeham, S.G., Amann, R., Freeman, K.H., Hopmans, E.C., Jørgensen, B.B., Putnam,
513 I.F., *et al*. (2007) Microbial ecology of the stratified water column of the Black Sea
514 as revealed by a comprehensive biomarker study. *Org Geochem* **38**: 2070-2097.
515 Wakeham, S.G., Lewis, C.M., Hopmans, E.C., Schouten, S., and Sinninghe Damsté, J.S.
516 (2003) Archaea mediate anaerobic oxidation of methane in deep euxinic waters of
517 the Black Sea. *Geochim Cosmochim Acta* **67**: 1359-1374.
518 Walker, M.C., and van der Donk, W.A. (2016) The many roles of glutamate in
519 metabolism. *J Ind Microbiol Biotechnol* **43**: 419-430.
520 Wang, R., Lin, J-Q., Liu, X-M., Pang, X., Zhang, C-J., Yang, C-L., *et al*. (2019) Sulfur
521 Oxidation in the Acidophilic Autotrophic *Acidithiobacillus* spp. *Front Microbiol* **9**:
522 3290.
523 Welsh, D.T. (2000) Ecological significance of compatible solute accumulation by
524 microorganisms from single cells to global climate. *FEMS Microbiol Rev* **24**: 263-
525 290.

526 Wernegreen, J.J. (2005) For better or worse: genomic consequences of intracellular
527 mutualism and parasitism. *Curr Opin Genet Dev* **15**: 572-583.
528 Wilcox, R.M., and Fuhrman, J.A. (1994) Bacterial viruses in coastal seawater: lytic rather
529 than lysogenic production. *Mar Ecol Prog Ser* **114**: 35-45.
530 Wolf, P.G., Biswas, A., Morales, S.E., Greening, C., and Gaskins, H.R. (2016)
531 $H_2$ metabolism is widespread and diverse among human colonic microbes. *Gut*
532 *Microbes* **7**: 235-245.
533 Yadav, S., Villanueva, L., Bale, N., Koenen, M., Hopmans, E.C., and Sinninghe Damsté,
534 J.S. (2020) Physiological, chemotaxonomic and genomic characterization of two
535 novel piezotolerant bacteria of the family *Marinifilaceae* isolated from sulfidic
536 waters of the Black Sea. *Syst Appl Microbiol* **43**: 126122.
537 Yano, Y., Nakayama, A., Ishihara, K., and Saito, H. (1998) Adaptive changes in
538 membrane lipids of barophilic bacteria in response to changes in growth
539 pressure. *Appl Environ Microbiol* **64**: 479-485.
540 Zhao, J-S., Dominic, Manno, D., and Hawari, J. (2009) *Psychrilyobacter atlanticus* gen.
541 nov., sp. nov., a marine member of the phylum *Fusobacteria* that produces $H_2$ and
542 degrades nitramine explosives under low temperature conditions. *Int J Syst Evol*
543 *Microbiol* **59**: 491-497.
544
545
546
547
548
549

**Table 1:** Core lipid composition of strains SD5$^T$, BL5 and *Psychrilyobacter atlanticus* JCM 14977$^T$ released by base hydrolysis; CLs = core lipids.

| | | BL5 | *P. atlanticus* JCM 14977$^T$ | SD5$^T$ | | |
|---|---|---|---|---|---|---|
| | | 0.1 MPa | | 0.1 MPa | 20 MPa | 30 MPa |
| **CLs** | $C_{11:0}$ | - | 0.5 | - | - | |
| | $C_{12:0}$ | 1.1 | 0.6 | 1.4 | 1.4 | |
| | $C_{12:1}$ | - | 0.2 | - | - | - |
| | $C_{13:0}$ | 0.3 | 0.2 | 0.4 | 0.5 | 0.6 |
| | $C_{14:1}$ ω6C | - | - | - | - | 0.9 |
| | $C_{14:1}$ ω 7C | 0.6 | - | 0.6 | 0.9 | |
| | $C_{14:1}$ ω 9C | 0.9 | - | 1.1 | 0.9 | 0.7 |
| | $C_{14:0}$ | **10.9** | 7.5 | **10.6** | 8.7 | 6.4 |
| | $C_{15:1}$ ω7C | 0.1 | - | 0.1 | 0.2 | 8.1 |
| | $C_{15:1}$ ω9C | 2.2 | - | 2.2 | 4.7 | 0.5 |
| | $C_{15:0}$ | 1.4 | 2.2 | 1.5 | 2.0 | 2.9 |
| | $C_{16:1}$ ω9C | **23.0** | **23.1** | **23.1** | **22.9** | **36.7** |
| | $C_{16:1}$ ω11C | 0.5 | - | 0.2 | 0.4 | 1.1 |
| | $C_{16:0}$ | **36.0** | **41.5** | **36.7** | **34.2** | **18.4** |
| | $C_{17:1}$ ω9C | 0.5 | 0.9 | 0.4 | 1.4 | 1.4 |
| | $C_{17:1}$ ω11C | 0.5 | 1.2 | 0.5 | 1.4 | 3.3 |
| | $C_{17:0}$ | 1.2 | 2.5 | 1.1 | 2.9 | 1.9 |
| | $C_{18:1}$ ω9C | 0.4 | 0.5 | 0.2 | 0.4 | 2.0 |
| | $C_{18:1}$ ω11C | 1.3 | 1.9 | 0.9 | 1.6 | 1.5 |
| | $C_{18:1}$ ω13C | - | - | 0.3 | - | |
| | $C_{18:0}$ | 1.5 | 1.6 | 0.9 | 2.0 | 2.7 |
| | Σ saturated FAs | 52.4 | 56.6 | 52.6 | 51.7 | 32.9 |
| | Σ unsaturated FAs | 30.0 | 27.8 | 29.6 | 34.8 | 56.2 |
| **Hydroxy FAs** | *β*-OH $C_{10:0}$ | 0.5 | 0.4 | 0.6 | 0.5 | - |
| | *β*-OH $C_{11:0}$ | 0.5 | 0.5 | 0.5 | 0.6 | 0.2 |
| | *β*-OH $C_{12:1}$ | 0.4 | - | 0.7 | 0.4 | 0.4 |
| | *β*-OH $C_{12:0}$ | 5.3 | 3.6 | 5.7 | 4.1 | 1.7 |
| | *β*-OH $C_{13:0}$ | 0.5 | 0.6 | 0.6 | 0.6 | 0.8 |
| | *β*-OH $C_{14:0}$ | 3.0 | 1.8 | 2.5 | 1.7 | 2.3 |
| | *β*-OH $C_{15:0}$ | 0.4 | 0.9 | 0.4 | 0.5 | 0.8 |
| | *β*-OH $C_{16:1}$ | 0.2 | - | 0.3 | 0.2 | 0.8 |
| | *β*-OH $C_{16:0}$ | 4.9 | 5.1 | 4.8 | 3.5 | 2.3 |
| | *β*-OH $C_{17:0}$ | 0.1 | 0.4 | 0.1 | 0.3 | 0.4 |
| | *β*-OH $C_{18:0}$ | 0.1 | 0.8 | 0.1 | 0.1 | - |
| | 3-Methoxy $C_{11:0}$ | 0.1 | - | 1.1 | 0.1 | - |
| | 3-Methoxy $C_{12:0}$ | 1.1 | - | 0.8 | 1.0 | - |
| | Di-hydroxy FAs | 0.6 | - | | 0.3 | - |

| | | | | | |
|---|---|---|---|---|---|
| Σ hydroxy FAs | 17.7 | 14.1 | 18.2 | 13.9 | 9.7 |

553

554

555

**Table 2:** The relative abundance of the intact polar lipids, grouped by headgroup. PEs, phosphatidylethanolamine; PGs, phosphatidylglycerol; PCs, phosphatidylcholine. The acyl moieties of the most abundant species of each polar head group are given.

| Polar head group | Acyl moieties of abundant species | SD5$^{T}$ (0.1 MPa) | SD5$^{T}$ (20 MPa) | SD5$^{T}$ (30 MPa) | BL5 |
|---|---|---|---|---|---|
| PEs | $C_{16:0}$, $C_{12:0}$<br>$C_{16:1}$, $C_{14:0}$<br>$C_{16:1}$, $C_{16:0}$<br>$C_{16:0}$, $C_{16:0}$ | 14.7 | 15.9 | 15.1 | 13.8 |
| PGs | $C_{16:0}$, $C_{15:1}$<br>$C_{16:1}$, $C_{14:0}$<br>$C_{16:1}$, $C_{16:0}$<br>$C_{16:1}$, $C_{16:1}$ | 18.6 | 24.4 | 50.8 | 18.4 |
| PCs | $C_{16:1}$, $C_{18:1}$<br>$C_{16:1}$, $C_{16:0}$<br>$C_{16:1}$, $C_{16:1}$ | 17.8 | 6.0 | 7.6 | 18.2 |
| Cardiolipins | $C_{16:0}$, $C_{16:1}$, $C_{16:0}$, $C_{12:0}$<br>$C_{16:0}$, $C_{16:1}$, $C_{16:1}$, $C_{14:0}$<br>$C_{16:0}$, $C_{16:1}$, $C_{16:0}$, $C_{15:1}$<br>$C_{16:0}$, $C_{16:1}$, $C_{16:1}$, $C_{16:0}$ | 23.7 | 28.6 | 18.7 | 21.2 |
| Lyso PEs | $C_{16:0}$ | 11.2 | 9.0 | 4.2 | 11.7 |
| Lyso PCs | $C_{16:0}$<br>$C_{18:0}$ | - | - | - | 3.8 |
| Lyso Cardiolipins | $C_{16:0}$, $C_{16:1}$, $C_{16:0}$<br>$C_{16:0}$, $C_{16:1}$, $C_{16:1}$ | 13.9 | 16.2 | 3.6 | 12.9 |

## Figure legends

**Fig. 1:** Fusobacteria in the Black Sea. **(A)** Water column concentration profiles of oxygen, $PO_4^{3-}$, $HS^-$ and $NH_4^+$ in the center of the gyre of the western basin (42 53.78' N 30 40.72') of the Black Sea (data from Sollai *et al*., 2019 and Suominen *et al*., 2021a). **(B)** Estimated abundance (expressed as the number of 16S rRNA gene copies $L^{-1}$) of the members of the phylum *Fusobacterial* and *Psychrilyobacter* spp. in the Black Sea water column. Data were obtained by sampling with Niskin bottles, filtration, DNA extraction, 16S rRNA gene amplicon sequencing and quantitative PCR, both using the same universal bacterial primers (see Yadav *et al*., 2020 and Villanueva *et al*., 2021). Note that the depth axis in (A) and (B) is not to scale. **(C)** Phylogenetic tree based on partial (~304 bp) 16S rRNA gene sequences obtained from SPM of the the Black Sea water at various depth (50-2000 m) and enrichment cultures. For reference, the full length 16S rRNA gene sequences of various type strains of the fusobacteria and those of the isolated strains $SD5^T$ and BL5 were used in the construction of the tree. The phylogenetic analysis shows the presence of seven clades within the phylum *Fusobacteria* in the Black Sea waters. The relative abundance of sequences affiliated with each clade (in % of all recovered 16S rRNA sequences) and their depth distribution is listed in parentheses. The sequences of the two isolated strains $SD5^T$, and BL5 and most of those obtained from the enrichment cultures were affiliated with clade V. The tree was constructed by the neighbor-joining method and rooted by using the *Streptobacillus felis* $131000547^T$ (HG421076) 16S rRNA gene sequence as an

outgroup. Numbers at nodes represent bootstrap values (based on 1,000 resamplings). The length of the bar indicates two nucleotide substitutions per 100 nucleotides.

**Fig. 2:** Cell morphology of strain SD5$^T$ grown at optimal growth conditions **(A)**, at 11 mM **(B, C, D)** and **(E)** 32 mM of sodium sulfide concentration **(C)** Sulfur granules are observed under phase contrast-microscope after 3 days of growth. Error bars refer to the standard error.

**Fig. 3:** Phylogenomic tree of strains SD5$^T$ and BL5, and their nearest phylogenetic neighbors affiliated with the phylum *Fusobacteria*. The tree was built by the maximum likelihood method using the Species TreeBuilder v.2.1.10 based on highly conserved concatenated protein sequences of 49 core, universal genes defined by COG (Clusters of Orthologous Groups) listed on the KBase server (Arkin *et al*., 2018). The tree was rooted by using *Ancylomarina subtilis* FA 102$^T$ (SHKN01000000) as an outgroup. The genome sequence accession numbers are shown between parentheses. Numbers at nodes represent bootstrap values (1 refers to 1000). The length of the bar indicates two nucleotide substitutions per 10 nucleotides.

**Fig. 4:** Doubling time of strain SD5$^T$ grown at various sulfide concentrations **(A)** and growth at optimal conditions (**B**; 23°C; 0.1 MPa, and pyruvate as carbon source) and **(C)** at 30 MPa with and without the addition of glutamate (other conditions unchanged). Key: $OD_{600}$ = optical density measured at 600 nm. Error bars refer to the standard error.

**Fig. 5:** Reconstruction of the central metabolic pathway of strain SD5$^T$ and BL5 based on different physiological analyses and by the presence of various genes identified in the genome sequence. Empty boxes indicate missing genes. IPP, isopentenyl pyrophosphate; PP Pathway, pentose phosphate pathway; geranyl-PP, geranyl pyrophosphate; GS, glutamine synthetase; glutamate synthase (GOGAT). Numbers identify genes according to the key in Supplementary Table S2.

# Figure 1

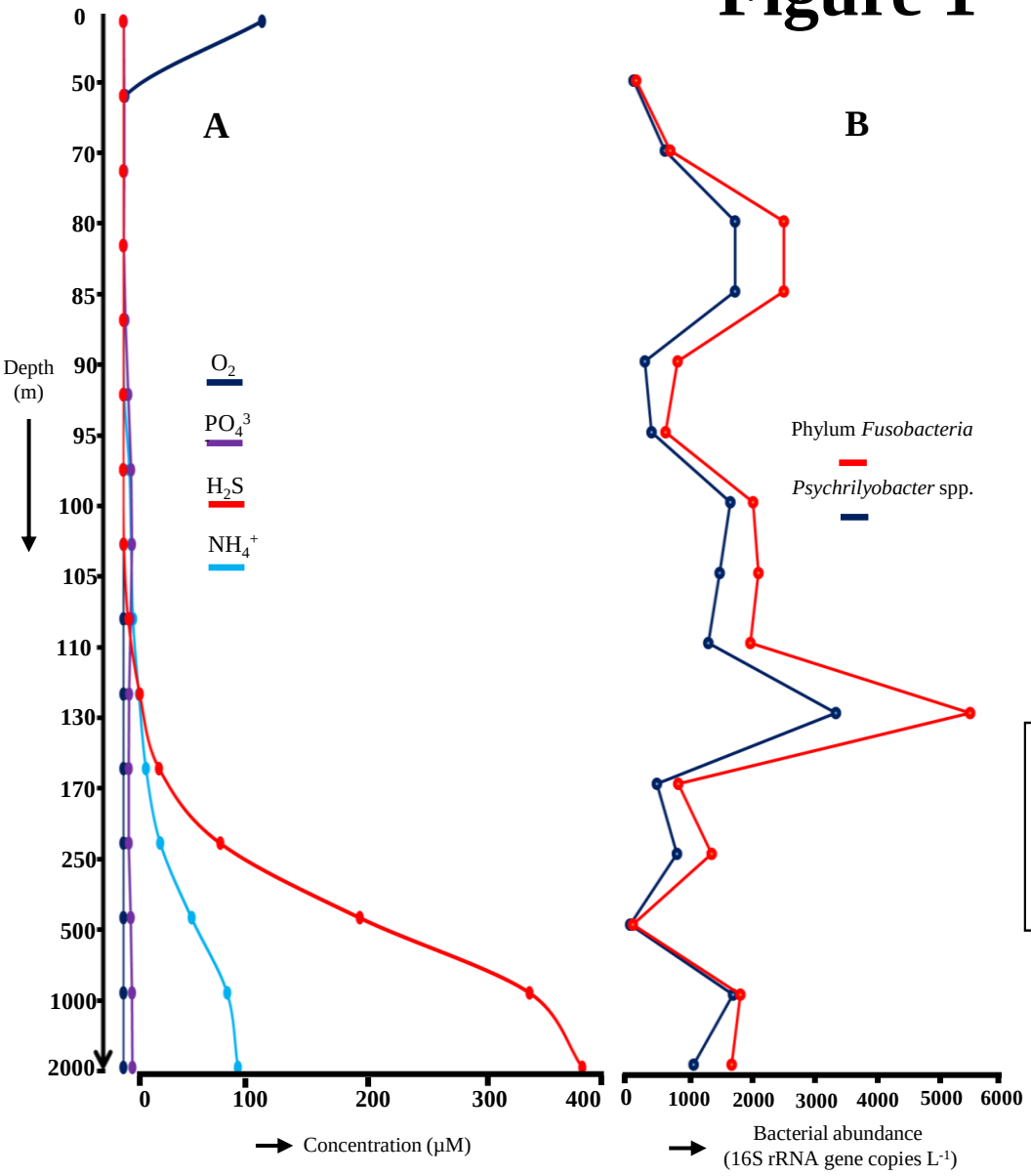
A
B
Depth (m)
0
50
70
80
85
90
95
100
105
110
130
170
250
500
1000
2000
$O_2$
$PO_4^{3}$
$H_2S$
$NH_4^{+}$
0
100
200
300
400
Concentration (µM)
Phylum *Fusobacteria*
*Psychrilyobacter* spp.
0
1000
2000
3000
4000
5000
6000
Bacterial abundance
(16S rRNA gene copies $L^{-1}$)

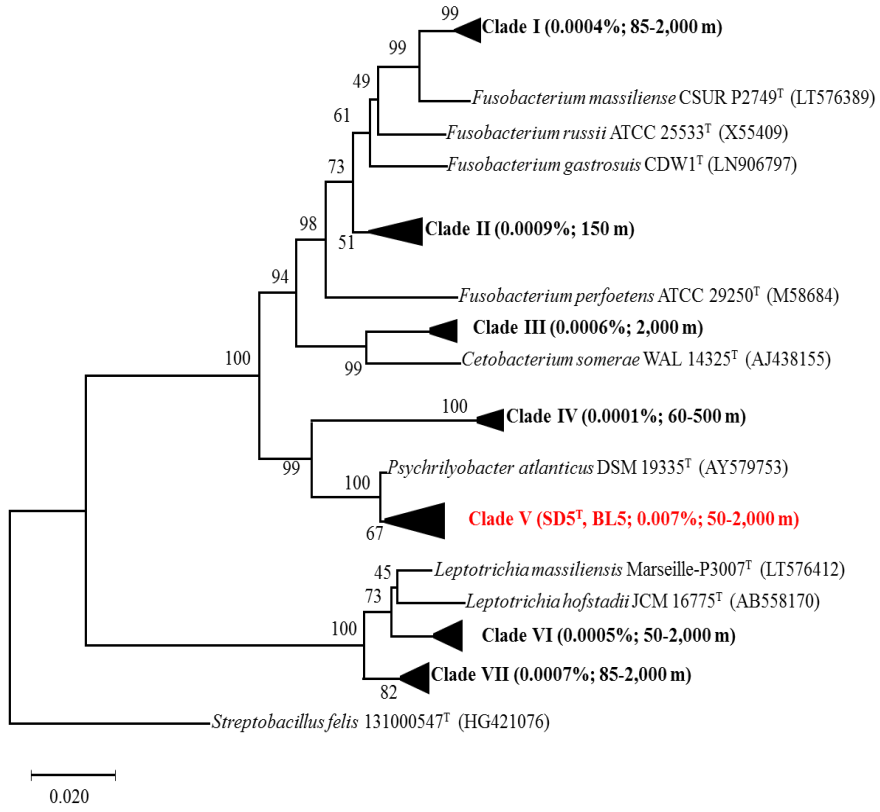
99
**Clade I (0.0004%; 85-2,000 m)**
99
49
*Fusobacterium massiliense* CSUR P2749$^{T}$ (LT576389)
61
*Fusobacterium russii* ATCC 25533$^{T}$ (X55409)
73
*Fusobacterium gastrosuis* CDW1$^{T}$ (LN906797)
98
51
**Clade II (0.0009%; 150 m)**
94
*Fusobacterium perfoetens* ATCC 29250$^{T}$ (M58684)
**Clade III (0.0006%; 2,000 m)**
100
99
*Cetobacterium somerae* WAL 14325$^{T}$ (AJ438155)
100
**Clade IV (0.0001%; 60-500 m)**
99
*Psychrilyobacter atlanticus* DSM 19335$^{T}$ (AY579753)
100
**Clade V (SD5$^{T}$, BL5; 0.007%; 50-2,000 m)**
67
45
*Leptotrichia massiliensis* Marseille-P3007$^{T}$ (LT576412)
73
*Leptotrichia hofstadii* JCM 16775$^{T}$ (AB558170)
100
**Clade VI (0.0005%; 50-2,000 m)**
**Clade VII (0.0007%; 85-2,000 m)**
82
*Streptobacillus felis* 131000547$^{T}$ (HG421076)
0.020

# Figure 2

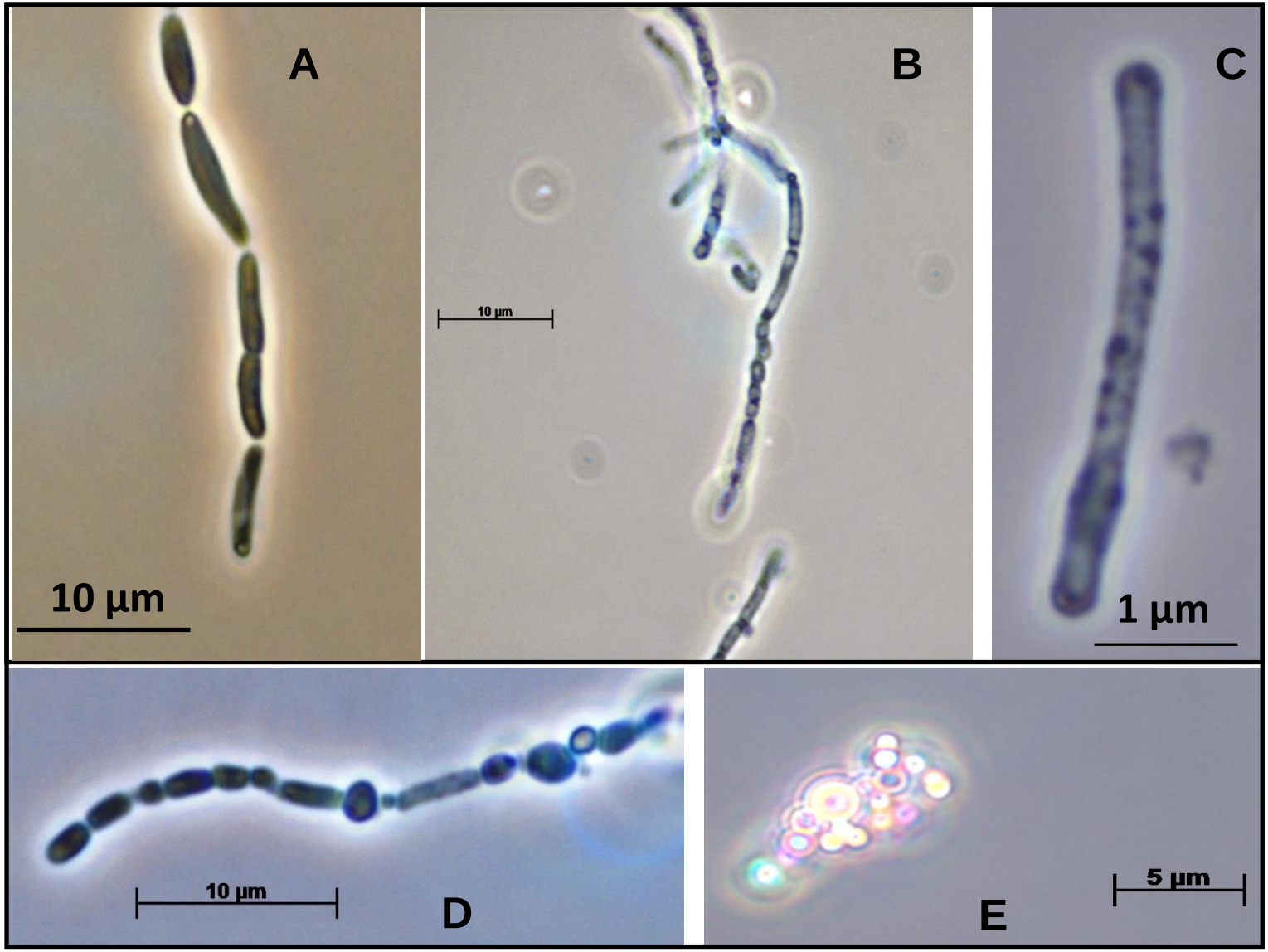

# Figure 3

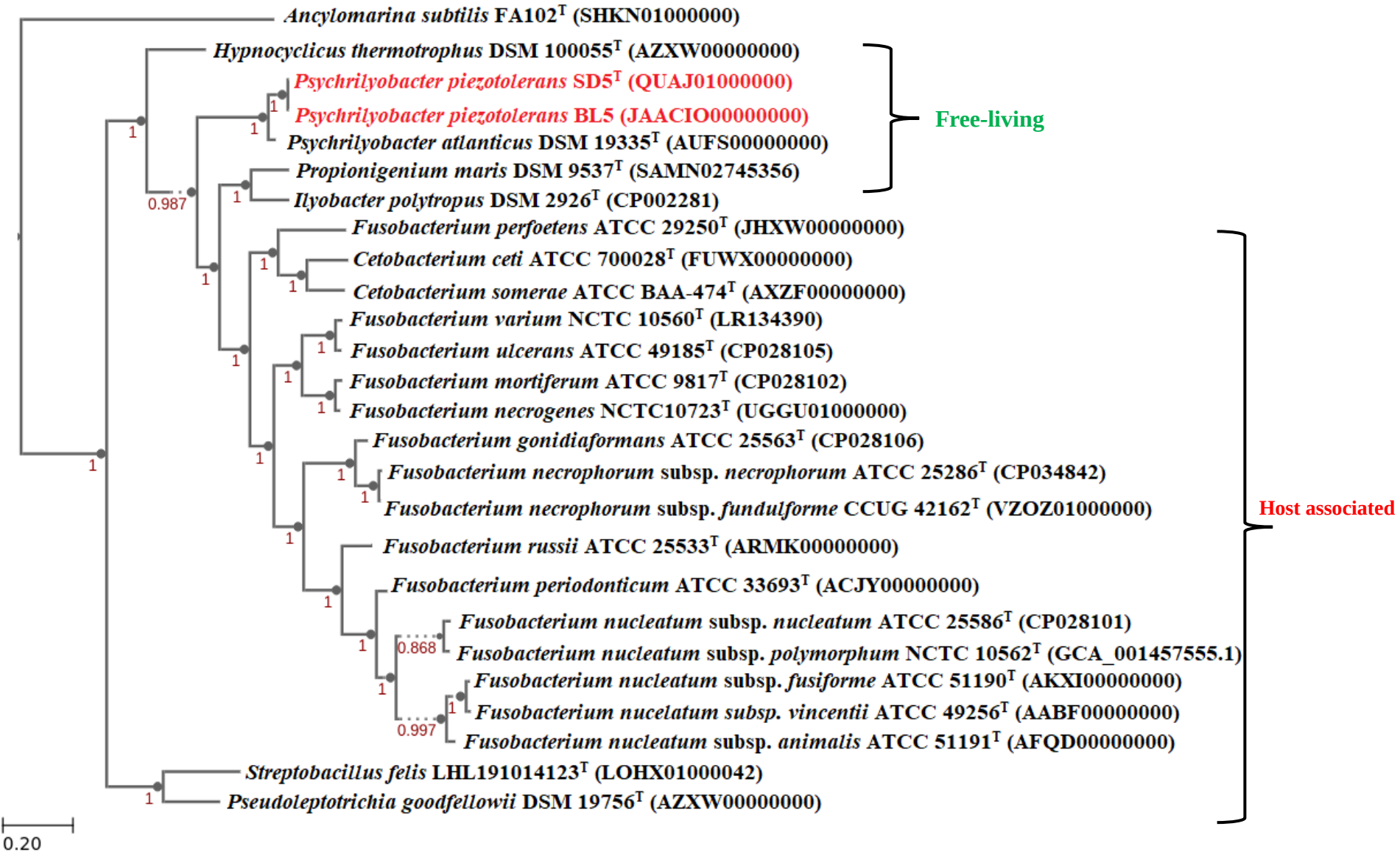
Ancylomarina subtilis FA102T (SHKN01000000)
Hypnocyclicus thermotrophus DSM 100055T (AZXW00000000)
Psychrilyobacter piezotolerans SD5T (QUAJ01000000)
Psychrilyobacter piezotolerans BL5 (JAACIO00000000)
Psychrilyobacter atlanticus DSM 19335T (AUFS00000000)
Propionigenium maris DSM 9537T (SAMN02745356)
Ilyobacter polytropus DSM 2926T (CP002281)
Free-living
Fusobacterium perfoetens ATCC 29250T (JHXW00000000)
Cetobacterium ceti ATCC 700028T (FUWX00000000)
Cetobacterium somerae ATCC BAA-474T (AXZF00000000)
Fusobacterium varium NCTC 10560T (LR134390)
Fusobacterium ulcerans ATCC 49185T (CP028105)
Fusobacterium mortiferum ATCC 9817T (CP028102)
Fusobacterium necrogenes NCTC10723T (UGGU01000000)
Fusobacterium gonidiaformans ATCC 25563T (CP028106)
Fusobacterium necrophorum subsp. necrophorum ATCC 25286T (CP034842)
Fusobacterium necrophorum subsp. fundulforme CCUG 42162T (VZOZ01000000)
Fusobacterium russii ATCC 25533T (ARMK00000000)
Fusobacterium periodonticum ATCC 33693T (ACJY00000000)
Fusobacterium nucleatum subsp. nucleatum ATCC 25586T (CP028101)
Fusobacterium nucleatum subsp. polymorphum NCTC 10562T (GCA_001457555.1)
Fusobacterium nucleatum subsp. fusiforme ATCC 51190T (AKXI00000000)
Fusobacterium nucelatum subsp. vincentii ATCC 49256T (AABF00000000)
Fusobacterium nucleatum subsp. animalis ATCC 51191T (AFQD00000000)
Host associated
Streptobacillus felis LHL191014123T (LOHX01000042)
Pseudoleptotrichia goodfellowii DSM 19756T (AZXW00000000)
0.987
0.868
0.997
0.20

# Figure 4

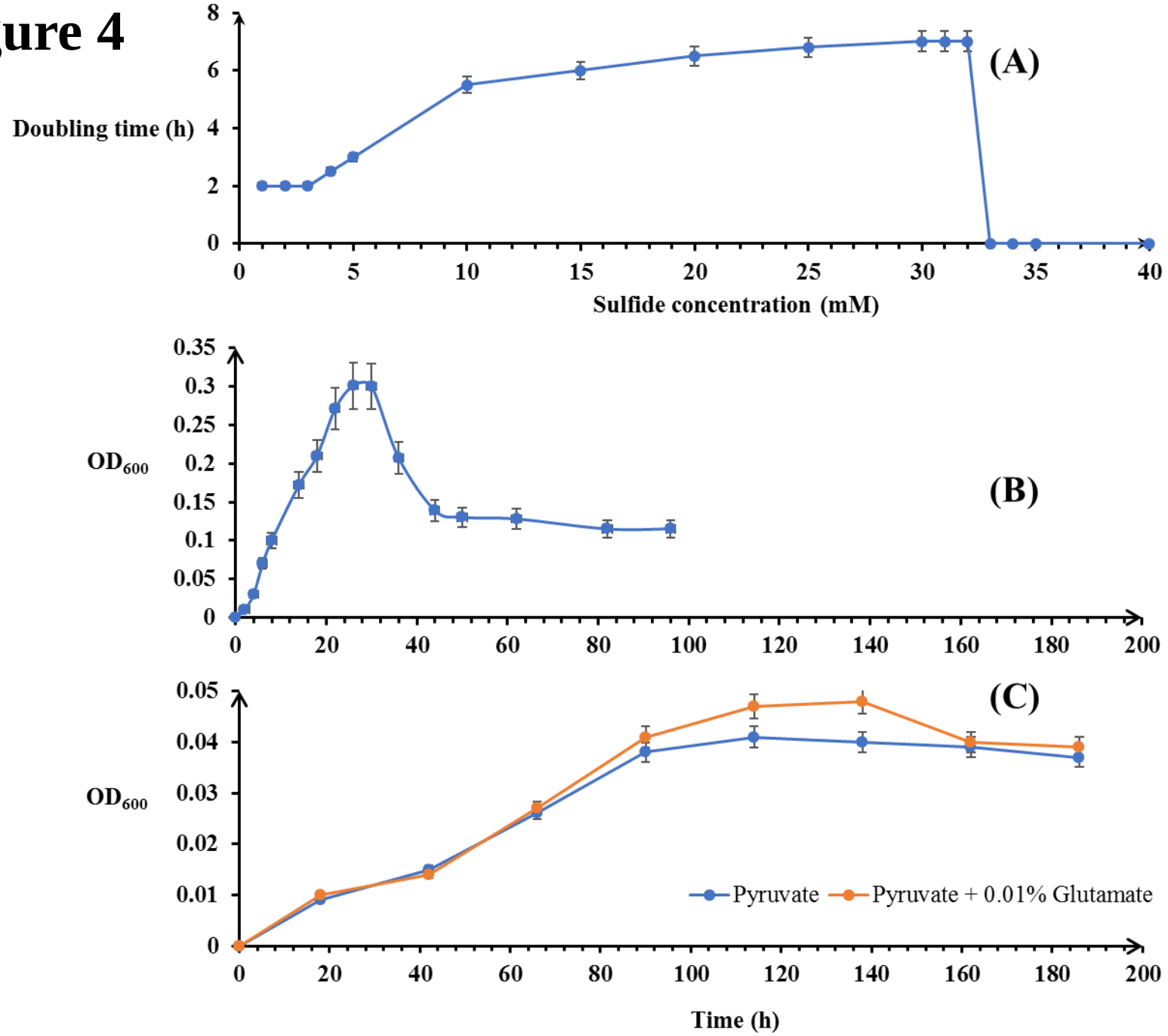
(A)
Doubling time (h)
Sulfide concentration (mM)
(B)
OD600
(C)
OD600
Time (h)
Pyruvate
Pyruvate + 0.01% Glutamate

# Figure 5

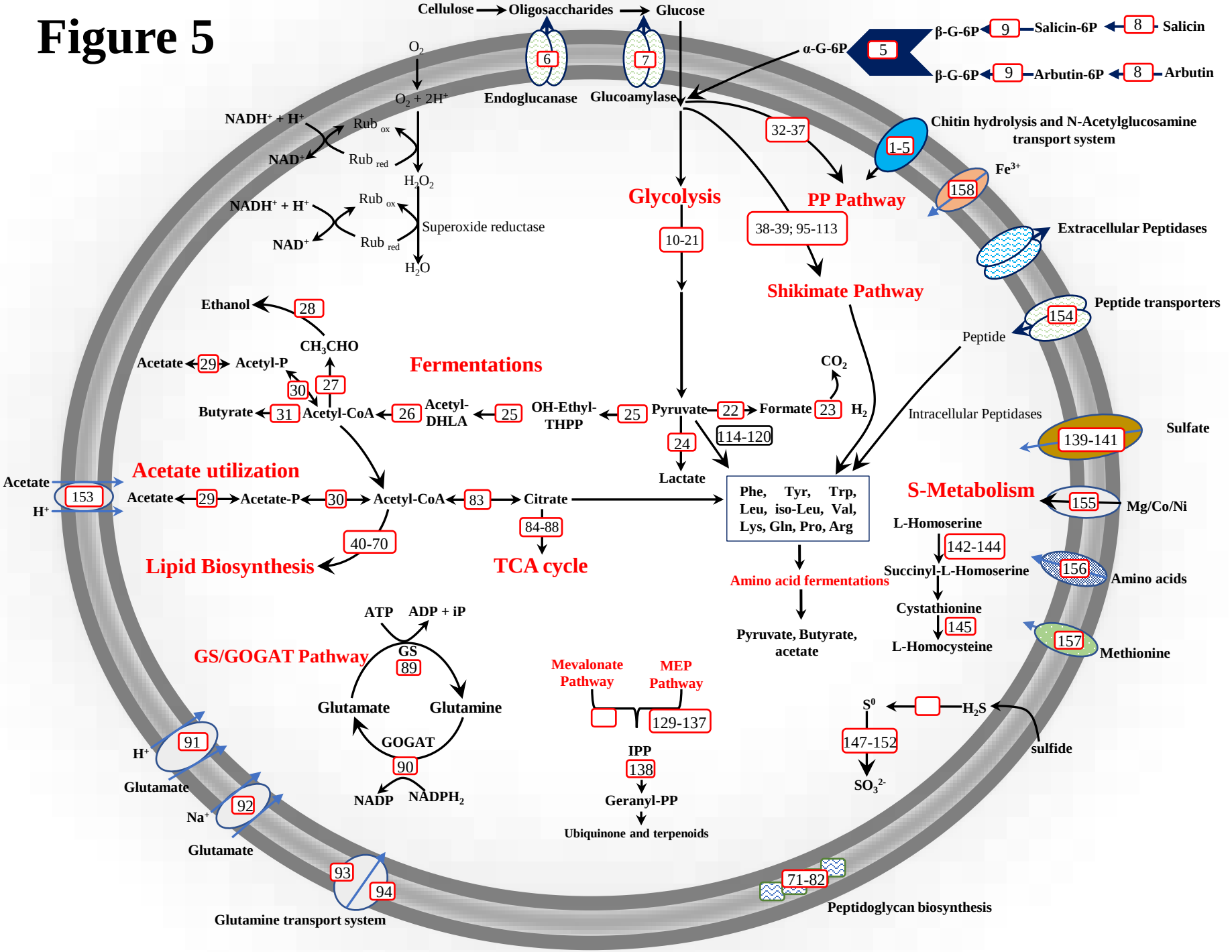
Cellulose
Oligosaccharides
Glucose
6
7
Endoglucanase
Glucoamylase
α-G-6P
5
β-G-6P
9
Salicin-6P
8
Salicin
β-G-6P
9
Arbutin-6P
8
Arbutin
O2
O2 + 2H+
NADH+ + H+
NAD+
Rub ox
Rub red
H2O2
Superoxide reductase
H2O
32-37
Chitin hydrolysis and N-Acetylglucosamine transport system
1-5
Fe3+
158
Glycolysis
PP Pathway
10-21
38-39; 95-113
Extracellular Peptidases
Shikimate Pathway
Peptide transporters
154
Peptide
Ethanol
28
CH3CHO
Acetate
29
Acetyl-P
30
27
Fermentations
CO2
H2
Butyrate
31
Acetyl-CoA
26
Acetyl-DHLA
25
OH-Ethyl-THPP
25
Pyruvate
22
Formate
23
Intracellular Peptidases
Sulfate
139-141
24
114-120
Lactate
Acetate
153
H+
Acetate utilization
Acetate
29
Acetate-P
30
Acetyl-CoA
83
Citrate
Phe, Tyr, Trp, Leu, iso-Leu, Val, Lys, Gln, Pro, Arg
S-Metabolism
155
Mg/Co/Ni
L-Homoserine
142-144
Succinyl-L-Homoserine
156
Amino acids
Cystathionine
145
L-Homocysteine
157
Methionine
40-70
Lipid Biosynthesis
84-88
TCA cycle
Amino acid fermentations
Pyruvate, Butyrate, acetate
ATP
ADP + iP
GS
89
GS/GOGAT Pathway
Glutamate
Glutamine
GOGAT
90
NADP
NADPH2
Mevalonate Pathway
MEP Pathway
129-137
IPP
138
Geranyl-PP
Ubiquinone and terpenoids
S0
H2S
147-152
SO32-
sulfide
H+
91
Glutamate
Na+
92
Glutamate
93
94
Glutamine transport system
71-82
Peptidoglycan biosynthesis

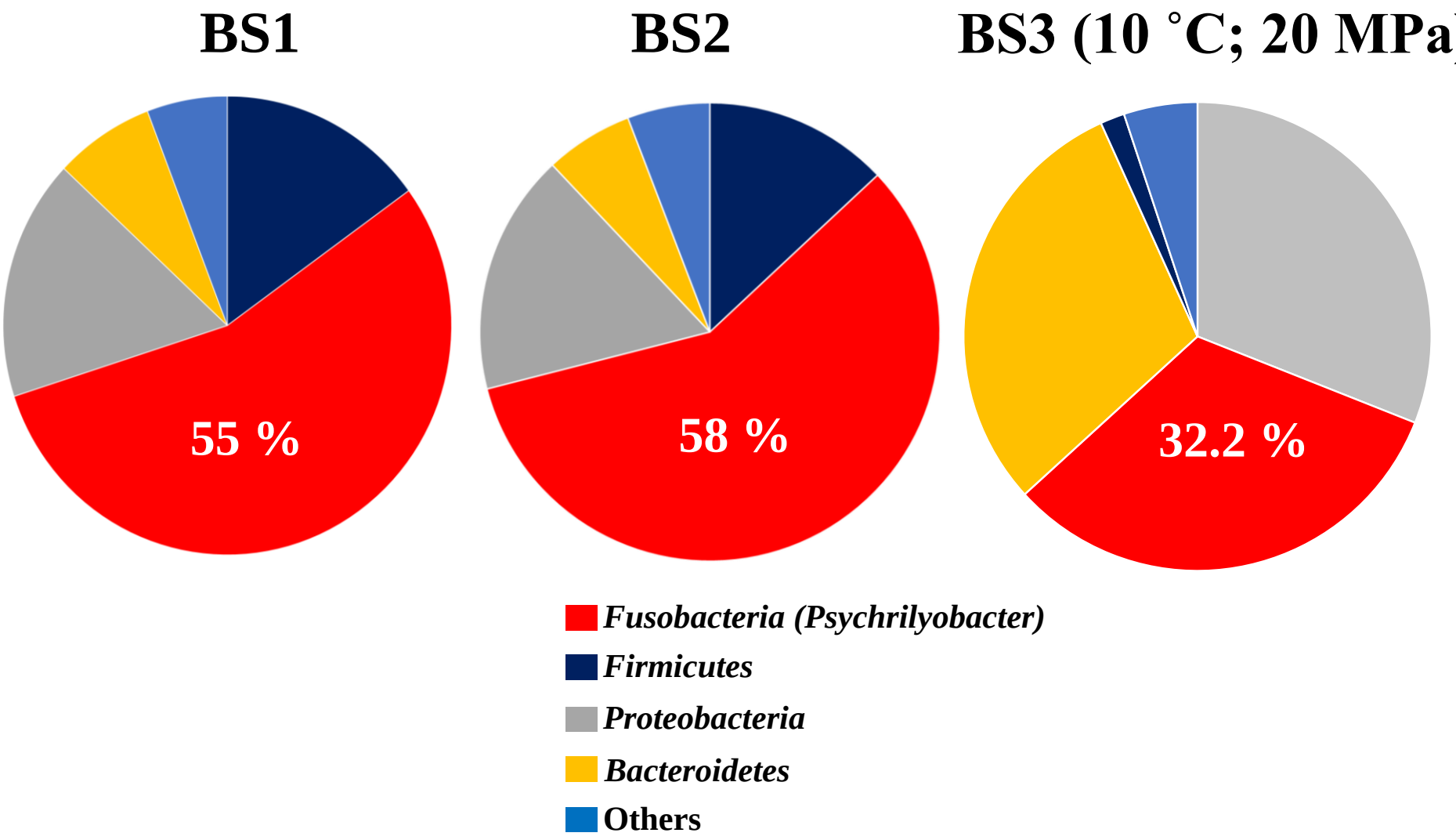


**Supplemental Fig. S1:** Relative abundance (in % of total bacterial and archaeal 16S rRNA gene sequences) of the *Psychrilyobacter* spp. and the composition of the rest of the microbial community in the enrichments using the growth media BS1, BS2 and BS3.

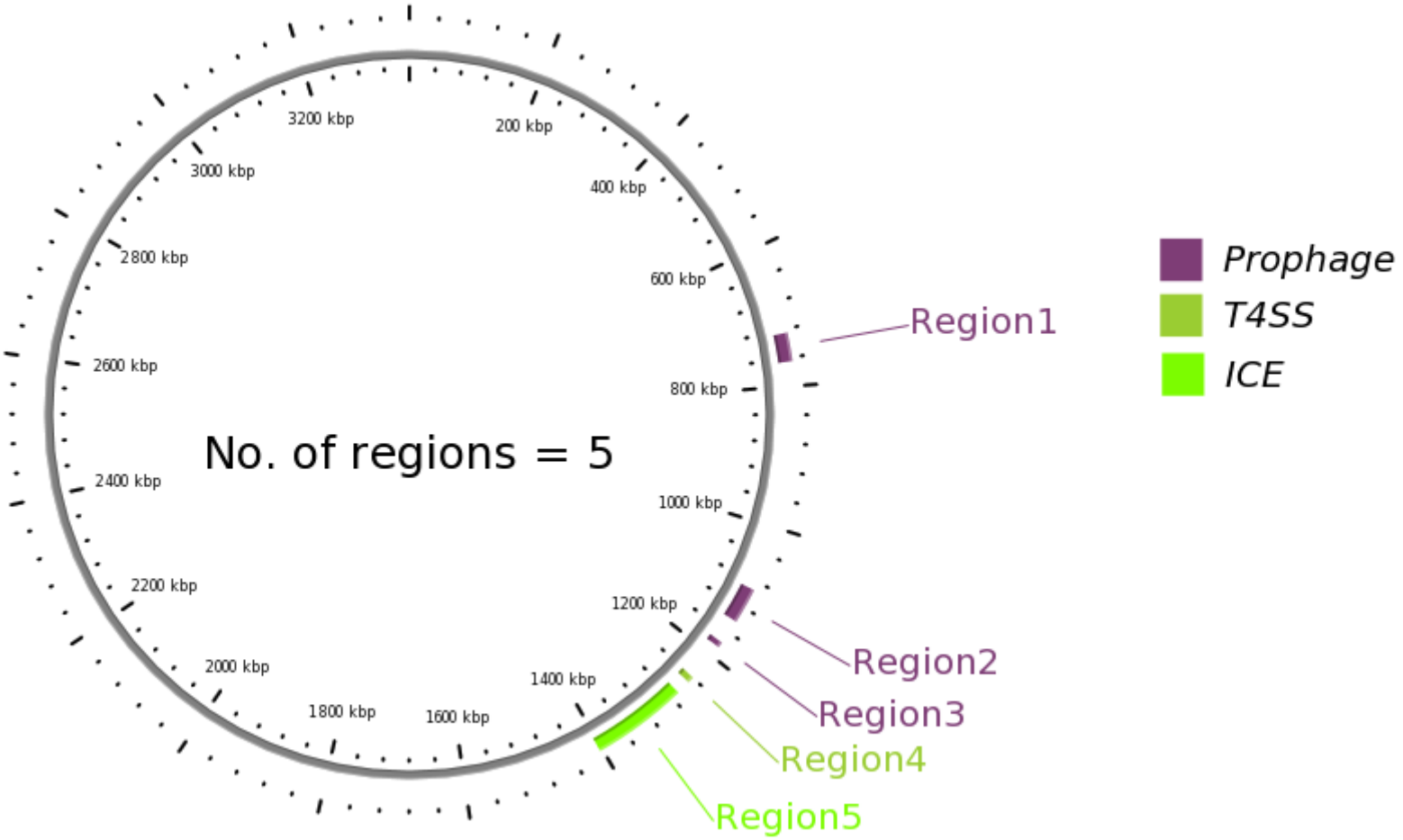


**Supplemental Fig. S2:** Putative virulence related regions identified in the genomes of strains SD5$^{T}$ and BL5.

# The physiology and metabolic properties of a novel, low-abundance *Psychrilyobacter* species isolated from the anoxic Black Sea shed light on its ecological role

**Running title**: Physiology of a novel *Psychrilyobacter* sp.

**Keywords**: *Fusobacteria*; *Psychrilyobacter*; Black Sea; Piezotolerance; Energy metabolism

Subhash Yadav[1], Michel Koenen[1], Nicole Bale[1],

Jaap S. Sinninghe Damsté[1,2], and Laura Villanueva[1,2]

[1]NIOZ Royal Netherlands Institute for Sea Research, Department of Marine Microbiology and Biogeochemistry, P.O. Box 59, 1797AB Den Burg, Texel, The Netherlands.

[2]Faculty of Geosciences. Department of Earth Sciences, Utrecht University., P.O. Box 80.021, 3508 TA Utrecht, The Netherlands.

*****Correspondence: Subhash Yadav, NIOZ Royal Netherlands Institute for Sea Research, Department of Marine Microbiology and Biogeochemistry, P.O. Box 59, 1797AB Den Burg, Texel, The Netherlands. Phone No. +31 222 369 427

E-mail: subhash.yadav@nioz.nl

## Experimental procedures

### Sampling sites, 16S rRNA gene amplicon sequencing and quantification

A sampling survey was conducted to collect water from the Black Sea in 2017 and 2018 on board of the *R/V* Pelagia as described elsewhere (Yadav *et al*., 2020). The study site was located at 42° 53.78' N 30° 40.72' E in the center of the gyre of the western basin. Water was collected with Niskin bottles under $N_2$ overpressure as described earlier (Yadav *et al*., 2020). To analyze the total prokaryotic diversity, DNA was extracted from both the water column from the Black Sea *in-situ* and from the enrichment cultures themselves, and further amplified for 16S rRNA gene amplicon sequencing as described earlier (Yadav *et al*., 2020). 16S rRNA gene amplicon data were analyzed by the Cascabel pipeline (Asbun *et al*., 2020) as described earlier (Yadav *et al*., 2020). Reads attributed to the *Fusobacteria* in the environmental samples and in the water sample kept in the lab to start enrichments were extracted by using Qiime (Caporaso *et al*., 2010) and, together with the 16S rRNA gene sequence of the isolated strain, used to construct a phylogenetic tree by using MEGA X as described earlier (Subhash *et al*., 2013). 16S rRNA gene copies were quantified using qPCR with the same primer pair as used for amplicon sequencing (515F, 806RB) as described earlier (van Grinsven *et al*., 2020). We estimated the absolute abundance of *Psychrilyobacter* spp. and other members of the phylum *Fusobacteria* by multiplying the total concentration of 16S rRNA gene copies per liter obtained by qPCR by the fractional abundance of *Fusobacteria*.

### Enrichment and isolation

Black Sea water collected during the 2017 and 2018 cruise was used for the subsequent enrichments in two different growth media. Growth medium 1 (BS1) contained (g $L^{-1}$, pH 7.0) cellulose (2.0); tryptone (2.0); yeast extract (1.0); $CaCl_2 \cdot 2H_2O$ (1.0), NaCl (20.0), $MgCl_2 \cdot 6H_2O$ (3.6), $MgSO_4 \cdot 7H_2O$ (4.3), KCl (0.5), $Na_2S.9H_2O$ (100 mg $L^{-1}$). Growth medium 2 (BS2) was prepared by diluting the medium BS1 for 10 times except for NaCl and $Na_2S.9H_2O$. Growth

medium 3 (BS3) was prepared by adding the sterilized Black Sea water (100 ml $L^{-1}$) in the BS2 with 400 µM of sulfide concentration to mimic the semi-natural compositions of the Black Sea. All medium components were sterilized by autoclaving at 121 ºC for 15 min. $MgCl_2 \cdot 6H_2O$ and $CaCl_2 \cdot 2H_2O$ were added from separately autoclaved stocks to prevent precipitation. All substrates were obtained from Sigma-Aldrich (Merck KGaA, Darmstadt, Germany). Enrichments were carried out in 110-mL serum bottles containing 50 mL of medium as described earlier (Yadav *et al*., 2020). Enrichments at elevated hydrostatic pressure (i.e., 20 MPa) were kept in a high-pressure cultivation device as described earlier (Yadav *et al*., 2020).

**Genome sequencing, assembly, annotations, and phylogenetic analysis**

Genomic DNA was isolated by the method of Marmur (1961) from pure cultures of the strains $SD5^T$ and BL5. Sequencing of the genome of both strains ($SD5^T$ and BL5) were performed at the CGEB-IMR (Dalhousie University, Canada), using an Illumina MiSeq (Illumina Inc) platform. Assembly of the raw sequencing data was performed by using the assembly service at PATRIC (Pathosystems Resource Integration Center; https://www.patricbrc.org/) server. Genome completeness was contamination were estimated by CheckM (Parks *et al*., 2015). Annotation of the assembled data was performed on prokka pipeline (Seemann, 2014) available on the DOE systems biology knowledgebase (KBase; Arkin *et al*., 2018), the Rapid Annotation Using Subsystem Technology (RAST; http://rast.nmpdr.org/rast.cgi; Brettin *et al*., 2015) and PATRIC (Pathosystems Resource Integration Center; https://www.patricbrc.org/; Wattam *et al*., 2017). BlastKOALA tool (Kanehisa *et al*., 2016) was used for the functional characterization of the genome sequence of strains $SD5^T$ and BL5. CRISPR arrays were identified with CRT (v. 1.1) (Bland *et al*., 2007). dbCAN meta server (Zhang *et al*., 2018) was used to identify the carbohydrate active enzymes in the genome sequence of strains $SD5^T$ and BL5. Putative virulence factors in the genomes were identified by using the VRprofile (Li et *al*., 2018). We used Species TreeBuilder v.2.1.10

to construct phylogenetic trees based on a set of 49 core, universal genes defined by COG (Clusters of Orthologous Groups) gene families (Price *et al*., 2010). Average nucleotide identity (ANI; Goris *et al*., 2007) and digital DNA-DNA hybridization (DDH; Richter and Rosselló-Móra, 2009) was performed by using the Kostas lab server (http://enve-mics.ce.gatech.edu/ani/) and genome-to-genome distance calculator (http://ggdc.dsmz.de/; Meier-Kolthoff *et al*., 2013), respectively. 16S rRNA gene amplicon sequencing data of the Black Sea water columns are deposited in NCBI as mentioned earlier (Yadav *et al*., 2020) and under Bioproject number PRJNA662699, PRJNA662698 and PRJNA681484. The NCBI accession number of the draft genome sequence of strains $SD5^T$ and BL5 are QUAJ00000000 and JAACIO000000000, respectively.

**Morphological, physiological, and biochemical analyses**

Morphological properties and other physiological tests such as growth at different temperatures, pH and NaCl were performed as described earlier (Shivani *et al*., 2015; 2016). Growth on organic substrates (D-glucose, glycerol, cellulose, chitin, cellobiose, sucrose, starch, pyruvate, acetate, L-glutamate and L-aspartic acid and L-lysine) was tested in a minimal medium described previously (Shivani *et al*., 2015; 2016). For chitin hydrolysis test, colloidal chitin was prepared as described earlier (Berger and Reynolds, 1988; Das *et al*., 2010). Colloidal chitin was used as the carbon source (0.5 g $L^{-1}$) in a growth medium (g $L^{-1}$, pH 7.0) which contained yeast extract (1.0); $CaCl_2 \cdot 2H_2O$ (1.0), NaCl (20.0), $MgCl_2 \cdot 6H_2O$ (3.6), $MgSO_4 \cdot 7H_2O$ (4.3), KCl (0.5), and $Na_2S.9H_2O$ (100 mg $L^{-1}$). Chitin hydrolysis was concluded as mentioned earlier (Das *et al*., 2010. Cellulose and starch hydrolysis was performed in the growth medium mentioned above with cellulose and starch as carbon source separately as described earlier (Cappuccino and Sherman, 1999; Shivani *et al*., 2015; 2016). Fermentation of various carbon sources (glucose, lactate, glycerol, xylose, galactose, cellobiose, maltose, lactose, aspartate, threonine, glutamate, and lysine) were tested as described previously

(Shivani *et al*., 2015; 2016). For validation of 2-*C*-methyl-D-erythritol 4-phosphate/1-deoxy-D-xylulose 5-phosphate (MEP/DOXP) and mevalonate pathway of isoprenoid biosynthesis in strain SD5$^T$ and BL5, MEP/DOXP pathway inhibitor (fosmidomycin (50 µg ml$^{-1}$) and mevalonate pathway inhibitor (simvastatin; 50 µg ml$^{-1}$) were used as described earlier (Shivani *et al*., 2016). Growth at elevated hydrostatic pressure (0.1 MPa-60 MPa) was tested in pressure vessels under strict anaerobic conditions as described previously (Yadav *et al*., 2020). Sulfide tolerance (0.1-40 mM) test was performed in the liquid medium which contained (g L$^{-1}$, pH 7.0) pyruvate (2.0); tryptone (2.0); yeast extract (1.0); $CaCl_2 \cdot 2H_2O$ (1.0), NaCl (20.0), $MgCl_2 \cdot 6H_2O$ (3.6), $MgSO_4 \cdot 7H_2O$ (4.3) and KCl (0.5). The sulfide solution was neutralized before adding to the medium as described earlier (Hansen and Veldkamp, 1973). Chemolithoautotrophic and chemolithoheterotrophic growth was tested as described earlier (Takai *et al*., 2009; Miroshnichenko *et al*., 2003). Growth on acetate (as a carbon source) and sulfate as terminal electron acceptor was tested in a growth medium which contained (g L$^{-1}$, pH 7.0) acetate (2.0); yeast extract (0.1); $CaCl_2 \cdot 2H_2O$ (1.0), NaCl (20.0), $MgCl_2 \cdot 6H_2O$ (3.6), $MgSO_4 \cdot 7H_2O$ (4.3); KCl (0.5) and trace elements (1 mL; Stams *et al*., 1993) as described earlier (Scholten and Stams, 2000). Various biochemical tests (casein hydrolysis, oxidase, and catalase activity) were carried out as described previously (Subhash *et al*., 2013; Shivani *et al*., 2015). Other enzymatic activities and biochemical test were determined with API 20 A kit (bioMerieux, France) according to the instructions of the manufacturer.

**Core lipid and intact polar lipid (IPL) analyses**

The core lipid of strains SD5$^T$, BL5 and *Psychrilyobacter atlanticus* JCM 14977$^T$ were analyzed on the culture grown in liquid medium with glucose as carbon source. Cells were harvested by centrifugation (5,000 g for 10 min at 25 °C) from late exponential phase of growth and core lipids were released by base hydrolysis and analyzed by gas chromatography/mass spectrometry (GC/MS), as described previously (van Vliet *et al*., 2020). Intact polar lipids

(IPLs) were extracted from freeze-dried biomass using a modified Bligh-Dyer procedure and were analyzed by high performance liquid chromatography-ion trap mass spectrometry (HPLC-ITMS) as described previously (Hazel and Williams, 1990).

**References**


Arkin, A.P., Cottingham, R.W., Henry, C.S., Harris, N.L., Stevens, R.L., Maslov, S., *et al*. (2018) KBase: The United States Department of Energy Systems Biology Knowledgebase. *Nat Biotechnol* **36**: 566.

Asbun, A., Besseling, M.A., Balzano, S., van Bleijswijk, J., Witte, H., Villanueva, L., and Engelmann, J.C. (2019) Cascabel: a flexible, scalable and easy-to-use amplicon sequence data analysis pipeline. *Front Genet* **11**:489357.

Berger, L. R., Reynolds, D. M. (1988) Colloidal chitin preparation. *Methods Enzymol* **161**, 140-142.

Bland, C., Ramsey, T.L., Sabree, F., Lowe, M., Brown, K., Kyrpides, N.C., *et al*. (2007) CRISPR recognition tool (CRT): a tool for automatic detection of clustered regularly interspaced palindromic repeats. *BMC Bioinformatics* **8**: 209.

Brettin, T., Davis, J.J., Disz, T., Edwards, R.A., Gerdes S, Olsen, G.J., *et al.* (2015). RASTtk: A modular and extensible implementation of the RAST algorithm for building custom annotation pipelines and annotating batches of genomes. *Sci Rep* **5**: 8365.

Caporaso, J.G., Kuczynski, J., Stombaugh, J., Bittinger, K., Bushman, F.D., Costello, E.K., *et al*. (2010) QIIME allows analysis of high-throughput community sequencing data. *Nat Methods* **7**: 335-336.

Cappuccino, J. G., Sherman, N. **(** 1999 **).** Microbiology: A Laboratory Manual. , 5th edn. Menlo Park, CA:: Benjamin Cummings.

Das, S. N., Sarma, P., Neeraja, C., Malati, N., Podile, A. R. (2010) Members of Gammaproteobacteria and Bacilli represent the culturable diversity of chitinolytic bacteria in chitin-enriched soils. *World J Microbiol Biotechnol* **26**, 1875-1881.

Goris, J., Konstantinidis, K.T., Klappenbach, J.A., Coenye, T., Vandamme, P., Tiedje, J.M., *et al*. (2007) DNA-DNA hybridization values and their relationship to whole-genome sequence similarities. *Int J Syst Evol Microbiol* **57**: 81-91.

Hansen, T.A., and Veldkamp, H. (1973) *Rhodopseudomonas sulfidophila*, nov. spec., a new species of the purple nonsulfur bacteria. *Archiv Microbiol* **92:** 45-58.

Hazel, J.R., and Williams, E.E. (1990) The role of alterations in membrane lipid composition in enabling physiological adaptation of organisms to their physical environment. *Prog Lipid Res* **29**: 167-227.

Kanehisa, M., Sato, Y., and Morishima, K. (2016). BlastKOALA and GhostKOALA: KEGG tools for functional characterization of genome and metagenome sequences. *J Mol Biol* **428**: 726-731.

Li, J., Tai, C., Deng, Z., Zhong, W., He, Y., and Ou, H.Y. (2018) VRprofile: gene-cluster-detection-based profiling of virulence and antibiotic resistance traits encoded within genome sequences of pathogenic bacteria. *Brief Bioinform* **19**: 566-574.

Maidak, B. L., Cole, J. R., Lilburn, T. G., Parker, C. T., Jr, Saxman, P. R., Farris, R. J., Garrity, G. M., Olsen, G. J., Schmidt, T. M., & Tiedje, J. M. (2001) The RDP-II (Ribosomal Database Project). *Nucleic Acids Res* **29**: 173-174.

Marmur, J.A. (1961) procedure for the isolation of deoxyribonucleic acid from microorganisms. *J Mol Biol* **3**: 208-218.

Meier-Kolthoff, J.P., Auch, A.F., Klenk, H.-P., and Göker, M. (2013) Genome sequence-based species delimitation with confidence intervals and improved distance functions. *BMC Bioinformatics* **14**: 60.

Miroshnichenko, M.L., L'Haridon, S., Jeanthon, C., Antipov, A.N., Kostrikina, N.A., Tindall, B.J., *et al*. (2003). *Oceanithermus profundus* gen. nov., sp. nov., a thermophilic, microaerophilic, facultatively chemolithoheterotrophic bacterium from a deep-sea hydrothermal vent. *Int J Syst Evol Microbiol* **53**: 747-752.

Parks, D.H., Imelfort, M., Skennerton, C.T., Hugenholtz, P., and Tyson, G.W. (2015) CheckM: assessing the quality of microbial genomes recovered from isolates, single cells, and metagenomes. *Genome Res* **25**: 1043-1055.

Price, M.N., Dehal, P.S., Arkin, A.P. (2010). FastTree 2 Approximately Maximum-Likelihood Trees for Large Alignments. *PLoS One* **5**: e9490.

Richter, M., and Rosselló-Móra, R. (2009) Shifting the genomic gold standard for the prokaryotic species definition. *Proc Natl Acad Sci USA* **106**: 19126-19131.

Scholten, J.C., Stams, A.J. (2000). Isolation and Characterization of Acetate-Utilizing Anaerobes from a Freshwater Sediment. *Microb Ecol* **40**: 292-299.

Seemann, T. (2014). Prokka: rapid prokaryotic genome annotation. *Bioinformatics* **30**: 2068 2069.

Shivani, Y., Subhash, Y., Sasikala, Ch., and Ramana, Ch.V. (2015) *Spirochaeta lutea* sp. nov., isolated from marine habitats and emended description of the genus *Spirochaeta*. *Syst Appl Microbiol* **38**: 110-114.

Shivani, Y., Subhash, Y., Sasikala, Ch., and Ramana, Ch.V. (2016) Description of *"Candidatus* Marispirochaeta associata*"* and reclassification of *Spirochaeta bajacaliforniensis*, *Spirochaeta smaragdinae* and *Spirochaeta sinaica* to a new genus *Sediminispirochaeta* gen. nov. as *Sediminispirochaeta bajacaliforniensis* comb. nov., *Sediminispirochaeta smaragdinae* comb. nov. and *Sediminispirochaeta sinaica* comb. nov. *Int J Syst Evol Microbiol* **66**: 5485-5492.

Stams, A.I.M., Vandijk, J.B., Dijkema, C., Plugge, C.M. (1993). Growth of syntrophic propionate-oxidizing bacteria with fumarate in the absence of methanogenic bacteria. *App1 Environ Microbiol* **59**: 1114-1119.

Subhash, Y., Sasikala, Ch., and Ramana, Ch.V. (2013) *Flavobacterium aquaticum* sp. nov., isolated from a water sample of a rice field. *Int. J Syst Evol Microbiol* **63**: 3463-3469.

Takai, K., Miyazaki, M., Hirayama, H., Nakagawa, S., Querellou, J., and Godfroy, A. (2009) Isolation and physiological characterization of two novel, piezophilic, thermophilic chemolithoautotrophs from a deep-sea hydrothermal vent chimney. *Environ Microbiol* **11**: 1983-1997.

van Grinsven, S., Sinninghe Damsté, J.S., Abdala, A.A,, Engelmann, J.C., Harrison, J., Villanueva, L. (2020). Methane oxidation in anoxic lake water stimulated by nitrate and sulfate addition. *Environ Microbiol* **22**: 766-782.

van Vliet, D.M., Lin, Y., Bale, N.J., Koenen M, Villanueva, L., Stams, A.J.M., and Sánchez-Andrea, I. (2020). *Pontiella desulfatans* gen. nov., sp. nov., and *Pontiella sulfatireligans* sp. nov., two marine anaerobes of the *Pontiellaceae* fam. nov. producing sulfated glycosaminoglycan-like exopolymers. *Microorganisms* **8**: 920.

Villanueva, L., von Meijenfeldt, F. A. B., Westbye, A.B., Yadav, S., Hopmans, E., Dutilh, B., and Damste, J.S.S. (2021) Bridging the membrane lipid divide: bacteria of the FCB group superphylum have the potential to synthesize archaeal ether lipids. *ISME J* **15**: 168-182.

Wattam, A.R., Davis, J.J., Assaf, R., Boisvert, S., Brettin, T., Bun, C. *et al.* (2017). Improvements to PATRIC, the all-bacterial Bioinformatics Database and Analysis Resource Center. *Nucleic Acids Res* **45**: D535-D542.

Yadav, S., Villanueva, L., Bale, N., Koenen, M., Hopmans, E.C., and Damsté, J.S.S. (2020) Physiological, chemotaxonomic and genomic characterization of two novel piezotolerant

bacteria of the family *Marinifilaceae* isolated from sulfidic waters of the Black Sea. *Syst Appl Microbiol* **43**: 126122.

Zhang, H., Yohe, T., Huang, L., Entwistle, S., Wu, P., Yang, Z., *et al*. (2018) dbCAN2: a meta server for automated carbohydrate-active enzyme annotation. *Nucleic Acids Res* **46**: W95-W101.

**Supplementary Table S1:** Comparative genomic analysis of strains SD5$^T$, BL5, and their closest phylogenetic neighbours affiliated with the phylum *Fusobacteria*.

| S. No. | Fusobacterial strains | Lifestyle | Genome Size (bp) | Genome Completeness (%) | %Contamination | G+C content | CDS | Proteins with functional assignments | tRNA | rRNA | Hypothetical proteins | CRISPR Repeats | Virulence factors | IPP Pathway | Antibiotic resistance genes | Accession number |
|---|---|---|---|---|---|---|---|---|---|---|---|---|---|---|---|---|
| 1 | Strain SD5$^T$ | F | 3,358,809 | 98.88 | 1.12 | 33.8 | 3256 | 2012 | 61 | 2 | 1244 | - | 3 | MEP/mevalonate | 33 | QUAJ00000000 |
| 2 | Strain BL5 | F | 3,344,081 | 98.88 | 1.12 | 33.8 | 3235 | 1966 | 63 | 2 | 1269 | - | 3 | MEP/mevalonate | 3 | JAACIO000000000 |
| 3 | *Psychrilyobacter atlanticus* DSM 19335$^T$ | F | 3,530,952 | 98.88 | 2.25 | 31.9 | 3347 | 2115 | 65 | 25 | 1232 | - | 1 | MEP | 30 | AUFS00000000 |
| 4 | *Propionigenium maris* DSM 9537$^T$ | F | 4,109,009 | 97.75 | 4.49 | 40.8 | 4115 | 1945 | 103 | 2 | 2170 | - | - | MEP | 28 | SAMN02745356 |
| 5 | *Ilyobacter polytropus* DSM 2926$^T$ | F | 3,132,314 | 100 | 0.00 | 34.3 | 3022 | 2238 | 79 | 26 | 784 | - | 2 | MEP | 27 | CP002281 |
| 6 | *Fusobacterium mortiferum* ATCC 9817$^T$ | H | 2,716,766 | 100 | 0.5 | 29.2 | 2664 | 1859 | 68 | 2 | 805 | 12 | 2 | MEP | 27 | CP028102 |
| 7 | *Fusobacterium necrogenes* NCTC 10723$^T$ | H | 2,015,236 | 100 | 0.2 | 29.2 | 1828 | 1351 | 66 | 13 | 477 | - | - | MEP | 26 | UGGU01000000 |
| 8 | *Fusobacterium ulcerans* ATCC 49185$^T$ | H | 3,537,675 | 100 | 0.00 | 30.5 | 3289 | 2117 | 57 | 14 | 1172 | 42 | 1 | MEP | 30 | CP028105 |
| 9 | *Fusobacterium gonidiaformans* ATCC 25563$^T$ | H | 1,678,881 | 100 | 0.00 | 32.7 | 1634 | 1243 | 50 | 12 | 391 | 84 | 1 | MEP | 24 | CP028106 |
| 10 | *Fusobacterium necrophorum* subsp. *funduliforme* CCUG 42162$^T$ | H | 2,124,940 | 100 | 0.00 | 34.9 | 2114 | 1507 | 50 | 17 | 607 | 43 | - | MEP | 24 | VZOZ01000000 |
| 11 | *Fusobacterium necrophorum* subsp. *necrophorum* ATCC 25286$^T$ | H | 2,678,415 | 100 | 0.00 | 34.0 | 2505 | 1781 | 51 | 12 | 1067 | 168 | - | MEP | 24 | CP034842 |
| 12 | *Fusobacterium russii* ATCC 25533$^T$ | H | 1,935,478 | 98.88 | 0.00 | 28.6 | 1742 | 1195 | 41 | 6 | 547 | - | 2 | MEP | 24 | ARMK00000000 |
| 13 | *Cetobacterium ceti* ATCC 700028$^T$ | H | 2,580,907 | 100 | 1.12 | 28.2 | 2538 | 1370 | 86 | 40 | 1168 | 19 | 3 | MEP | 27 | FUWX00000000 |
| 14 | *Fusobacterium varium* NCTC 10560$^T$ | H | 3,302,398 | 98.31 | 2.25 | 29.3 | 3519 | 2520 | 58 | 14 | 999 | 58 | 1 | MEP | 33 | LR134390 |

| | | | | | | | | | | | | | | | |
|---|---|---|---|---|---|---|---|---|---|---|---|---|---|---|---|
| 15 | *Cetobacterium somerae* ATCC BAA-474$^T$ | H | 3,064,648 | 98.88 | 0.00 | 28.6 | 2850 | 1685 | 29 | 4 | 1165 | - | 1 | MEP | 32 | AXZF00000000 |
| 16 | *Fusobacterium periodonticum* ATCC 33693$^T$ | H | 2,615,003 | 100 | 1.30 | 27.4 | 2453 | 1469 | 45 | 7 | 984 | - | - | MEP | 26 | ACJY00000000 |
| 17 | *Fusobacterium nucleatum* subsp. *polymorphum* NCTC 10562$^T$ | H | 2,455,060 | 100 | 0.00 | 27.0 | 2351 | 1567 | 47 | 15 | 784 | 30 | 3 | MEP | 24 | GCA_001457555.1 |
| 18 | *Fusobacterium perfoetens* ATCC 29250$^T$ | H | 2,102,197 | 100 | 0.5 | 25.9 | 1944 | 1238 | 41 | 15 | 706 | - | - | MEP | 27 | JHXW00000000 |
| 19 | *Hypnocyclicus thermotrophus* DSM 100055$^T$ | H | 2,218,931 | 100 | 0.00 | 24.8 | 2053 | 1241 | 61 | 3 | 812 | 44 | 2 | MEP | 25 | SOBG01000000 |
| 20 | *Fusobacterium nucleatum* subsp. *nucleatum* ATCC 25586$^T$ | H | 2,180,101 | 100 | 0.00 | 27.1 | 2065 | 1593 | 47 | 5 | 472 | 18 | 2 | MEP | 24 | CP028101 |
| 21 | *Fusobacterium nucleatum* subsp. *fusiforme* ATCC 51190$^T$ | H | 1,837,113 | 100 | 0.00 | 27.2 | 1723 | 1328 | 45 | 11 | 395 | - | 1 | MEP | 23 | AKXI00000000 |
| 22 | *Fusobacterium nucleatum* subsp. *vincentii* ATCC 49256$^T$ | H | 2,118,259 | 94.92 | 1.12 | 27.3 | 2296 | 1600 | 44 | 7 | 696 | - | 1 | MEP | 28 | AABF00000000 |
| 23 | *Fusobacterium nucleatum* subsp. *animalis* ATCC 51191$^T$ | H | 2,270,170 | 94.38 | 0.56 | 27.5 | 2401 | 1658 | 42 | 5 | 743 | - | 3 | MEP | 30 | AFQD00000000 |
| 24 | *Pseudoleptotrichia goodfellowii* DSM 19756$^T$ | H | 2,280,962 | 100 | 2.25 | 31.6 | 2257 | 1392 | 38 | 7 | 436 | - | 2 | MEP | 20 | AZXW00000000 |
| 25 | *Streptobacillus felis* LHL191014123$^T$ | H | 1,386,907 | 98.6 | 0.00 | 26.3 | 1406 | 970 | 37 | 2 | 680 | - | 2 | MEP | 24 | LOHX01000042 |

bp, base pair; F, free-living; H, host associated; -, not detected; IPP, isopentenyl pyrophosphate; MEP, 2-*C*-methyl-D-erythritol 4-phosphate.

**Supplementary Table S2:** List of various genes identified in the genome sequence of strains SD5$^T$ and BL5.

| S.No. | Genes |
|---|---|
| | **Chitin hydrolysis and N-Acetylglucosamine transport** |
| 1 | PTS system, N-acetylglucosamine-specific IIA component (EC 2.7.1.69) / PTS system, N-acetylglucosamine-specific IIB component (EC 2.7.1.69) / PTS system, N-acetylglucosamine-specific IIC component (EC 2.7.1.69) |
| 2 | N-Acetyl-D-glucosamine ABC transport system, permease protein 1 |
| 3 | N-Acetyl-D-glucosamine ABC transport system, permease protein 2 |
| 4 | N-acetylglucosamine-6-phosphate deacetylase (EC 3.5.1.25) |
| 5 | Glucosamine-6-phosphate deaminase (EC 3.5.99.6) |
| | **Cellulose hydrolysis** |
| 6 | Endoglucanase (EC 3.2.1.4) |
| 7 | Glucoamylase (EC 3.2.1.3) |
| 8 | PTS system, sugar-specific IIA component [EC:2.7.1.-] |
| 9 | 6-Phospho-beta-glucosidase [EC:3.2.1.86] |
| 10 | Glucose-6-phosphate isomerase [EC:5.3.1.9] |
| | **Glycolysis/Glyconeogenesis** |
| 11 | Glucokinase [EC:2.7.1.2] |
| 12 | Glucose-6-phosphate isomerase [EC:5.3.1.9] |
| 13 | 6-Phosphofructokinase 1 [EC:2.7.1.11] |
| 14 | Fructose-1,6-bisphosphatase, GlpX type (EC 3.1.3.11) |
| 15 | Fructose-bisphosphate aldolase, class II [EC:4.1.2.13] |
| 16 | Triosephosphate isomerase (TIM) [EC:5.3.1.1] |
| 17 | Glyceraldehyde 3-phosphate dehydrogenase [EC:1.2.1.12] |
| 18 | Phosphoglycerate kinase [EC:2.7.2.3] |
| 19 | 2,3-Bisphosphoglycerate-independent phosphoglycerate mutase [EC:5.4.2.12]/ Probable phosphoglycerate mutase [EC:5.4.2.12] |
| 20 | Enolase [EC:4.2.1.11] |
| 21 | Pyruvate kinase [EC:2.7.1.40] |
| | **Fermentation** |
| 22 | Pyruvate formate-lyase (EC 2.3.1.54) |
| 23 | Formate dehydrogenase chain D (EC 1.2.1.2) |
| 24 | L-lactate dehydrogenase (EC 1.1.2.3) |
| 25 | Pyruvate dehydrogenase E1 component [EC:1.2.4.1] |
| 26 | Pyruvate dehydrogenase E2 component (dihydrolipoamide acetyltransferase) [EC:2.3.1.12] |
| 27 | Acetaldehyde dehydrogenase (EC 1.2.1.10) |
| 28 | Alcohol dehydrogenase (EC 1.1.1.1) |
| 29 | Acetate kinase (EC 2.7.2.1) |
| 30 | Phosphate acetyltransferase (EC 2.3.1.8) |
| 31 | Butyrate-acetoacetate CoA-transferase subunit A (EC 2.8.3.9) |
| | **Pentose phosphate pathway** |
| 32 | Glucose-6-phosphate 1-dehydrogenase [EC:1.1.1.49 1.1.1.363] |
| 33 | Glucose-6-phosphate 1-dehydrogenase [EC:1.1.1.49 1.1.1.363] |
| 34 | 6-Phosphogluconolactonase [EC:3.1.1.31] |
| 35 | 6-Phosphogluconate dehydrogenase [EC:1.1.1.44 1.1.1.343] |
| 36 | Ribose 5-phosphate isomerase A [EC:5.3.1.6] |
| 37 | Ribose-phosphate pyrophosphokinase [EC:2.7.6.1] |

| | |
|---|---|
| 38 | Transketolase [EC:2.2.1.1] |
| 39 | Ribulose-phosphate 3-epimerase [EC:5.1.3.1] |
| | **Lipid Biosynthesis** |
| 40 | Acetyl-CoA carboxylase / biotin carboxylase 1 [EC:6.4.1.2 6.3.4.142.1.3.15] |
| 41 | [Acyl-carrier-protein] S-malonyltransferase [EC:2.3.1.39] |
| 42 | 3-Oxoacyl-[acyl-carrier-protein] synthase III [EC:2.3.1.180] |
| 43 | 3-Oxoacyl-[acyl-carrier-protein] synthase II [EC:2.3.1.179] |
| 44 | 3-Oxoacyl-[acyl-carrier protein] reductase [EC:1.1.1.100] |
| 45 | 3-Hydroxyacyl-[acyl-carrier-protein] dehydratase [EC:4.2.1.59] |
| 46 | Enoyl-[acyl-carrier protein] reductase II [EC:1.3.1.9] |
| 47 | Enoyl-[acyl-carrier protein] reductase / trans-2-enoyl-CoA reductase (NAD+) [EC:1.3.1.9 1.3.1.44] |
| 48 | Acyl-[acyl-carrier-protein] desaturase [EC:1.14.19.2 1.14.19.111.14.19.26] |
| 49 | Long-chain acyl-CoA synthetase [EC:6.2.1.3] |
| 50 | acyl-coenzyme A thioesterase 1/2/4 [EC:3.1.2.2] |
| | **Phosphatidylethanolamine biosynthesis** |
| 51 | Phosphatidate cytidylyltransferase [EC:2.7.7.41] |
| 52 | Phosphatidylserine decarboxylase [EC:4.1.1.65] |
| 53 | CDP-diacylglycerol---serine O-phosphatidyltransferase [EC:2.7.8.8] |
| | **Glycerophospholipid metabolism** |
| 54 | Glycerol-3-phosphate dehydrogenase [EC:1.1.9.4] |
| 55 | Glycerol-3-phosphate dehydrogenase (EC 1.1.5.3) |
| 56 | Lipid A biosynthesis lauroyl acyltransferase (EC 2.3.1.-) |
| 57 | 4-Hydroxybutyrate: acetyl-CoA CoA transferase (EC 2.3.1.-) |
| 58 | 1-Acyl-sn-glycerol-3-phosphate acyltransferase (EC 2.3.1.51) |
| 59 | Phosphatidate cytidylyltransferase (EC 2.7.7.41) |
| 60 | CDP-diacylglycerol--serine O-phosphatidyltransferase (EC 2.7.8.8) |
| 61 | CDP-diacylglycerol--glycerol-3-phosphate 3-phosphatidyltransferase (EC 2.7.8.5) |
| 62 | Phosphatidylglycerophosphatase A (EC 3.1.3.27) |
| 63 | Cardiolipin synthase (EC 2.7.8.-) bacterial type ClsA |
| 64 | D-glycero-D-manno-heptose 1,7-bisphosphate phosphatase (EC 3.1.1.-) |
| 65 | Diacylglycerol kinase (EC 2.7.1.107) |
| 66 | Phosphatidylserine decarboxylase (EC 4.1.1.65) |
| 67 | Lysophospholipase (EC 3.1.1.5); Monoglyceride lipase (EC 3.1.1.23); putative |
| 68 | Glycerophosphoryl diester phosphodiesterase (EC 3.1.4.46) |
| 69 | Ethanolamine ammonia-lyase light chain (EC 4.3.1.7) |
| 70 | Ethanolamine ammonia-lyase heavy chain (EC 4.3.1.7) |
| | **Peptidoglycan biosynthesis** |
| 71 | UDP-N-acetylglucosamine 1-carboxyvinyltransferase (EC 2.5.1.7) |
| 72 | UDP-N-acetylmuramate--alanine ligase (EC 6.3.2.8) |
| 73 | UDP-N-acetylmuramoylalanine--D-glutamate ligase (EC 6.3.2.9) |
| 74 | UDP-N-acetylmuramoyl-L-alanyl-D-glutamate--2,6-diaminopimelate ligase (EC 6.3.2.13) |
| 75 | D-alanine--D-alanine ligase (EC 6.3.2.4) |
| 76 | UDP-N-acetylmuramoyl-tripeptide--D-alanyl-D-alanine ligase (EC 6.3.2.10) |
| 77 | Phospho-N-acetylmuramoyl-pentapeptide-transferase (EC 2.7.8.13) |
| 78 | Undecaprenyl-diphosphatase (EC 3.6.1.27) |
| 79 | UDP-N-acetylglucosamine--N-acetylmuramyl-(pentapeptide) pyrophosphoryl-undecaprenol N-acetylglucosamine transferase (EC 2.4.1.227) |
| 80 | Lipid carrier: UDP-N-acetylgalactosaminyltransferase (EC 2.4.1.-) |

| | |
|---|---|
| 81 | Multimodular transpeptidase-transglycosylase (EC 2.4.1.129) (EC 3.4.-.-) |
| 82 | Peptidoglycan D, D-transpeptidase MrdA (EC 3.4.16.4) |
| | **Citric acid cycle** |
| 83 | Citrate synthase (si) (EC 2.3.3.1) |
| 84 | Aconitate hydratase (EC 4.2.1.3) |
| 85 | Isocitrate dehydrogenase [NAD] (EC 1.1.1.41) |
| 85a | 2-Oxoglutarate ferredoxin oxidoreductase (EC 1.2.7.-) |
| 86 | Succinate dehydrogenase (ubiquinone) flavoprotein subunit [EC:1.3.5.1] |
| 87 | Fumarate hydratase (EC 4.2.1.2) |
| 88 | Citrate lyase (EC 4.1.3.6) |
| | **GS-GOGAT Pathway** |
| 89 | Glutamate synthase [NADPH] small chain (EC 1.4.1.13) |
| 90 | Glutamine synthetase type III, GlnN (EC 6.3.1.2) |
| | **Glutamate symport** |
| 91 | Proton-glutamate symport protein |
| 92 | Sodium-glutamate symport protein |
| 93 | Putative glutamine transport system permease |
| 94 | Glutamine transport ATP-binding protein GlnQ (TC 3.A.1.3.2) |
| | **Shikimate Pathway and aromatic acid biosynthesis** |
| 95 | 3-Deoxy-7-phosphoheptulonate synthase [EC:2.5.1.54] |
| 96 | 3-Dehydroquinate synthase [EC:4.2.3.4] |
| 97 | 3-Dehydroquinate dehydratase I [EC:4.2.1.10] |
| 98 | Shikimate dehydrogenase [EC:1.1.1.25] |
| 99 | Shikimate kinase [EC:2.7.1.71] |
| 100 | 3-Phosphoshikimate 1-carboxyvinyltransferase [EC:2.5.1.19] |
| 101 | Chorismate synthase [EC:4.2.3.5] |
| 102 | Chorismate mutase [EC:5.4.99.5] |
| 103 | Aromatic-amino-acid transaminase [EC:2.6.1.57] |
| 104 | Prephenate dehydratase [EC:4.2.1.51] |
| 105 | Prephenate dehydrogenase [EC:1.3.1.12] |
| 106 | Histidinol-phosphate aminotransferase [EC:2.6.1.9] |
| 107 | Aromatic-amino-acid transaminase [EC:2.6.1.57] |
| 108 | Anthranilate synthase / indole-3-glycerol phosphate synthase [EC:4.1.3.27 4.1.1.48] |
| 109 | Anthranilate phosphoribosyltransferase [EC:2.4.2.18] |
| 110 | Anthranilate synthase / indole-3-glycerol phosphate synthase / phosphoribosylanthranilate isomerase [EC:4.1.3.27 4.1.1.48 5.3.1.24] |
| 111 | Anthranilate synthase / indole-3-glycerol phosphate synthase [EC:4.1.3.27 4.1.1.48] |
| 112 | Tryptophan synthase alpha chain [EC:4.2.1.20] |
| 113 | Tryptophan synthase beta chain [EC:4.2.1.20] |
| | **Leucine, isoleucine and valine biosynthesis** |
| 114 | Acetolactate synthase I/II/III large subunit [EC:2.2.1.6] |
| 115 | Ketol-acid reductoisomerase [EC:1.1.1.86] |
| 116 | Dihydroxy-acid dehydratase [EC:4.2.1.9] |
| 117 | Branched-chain amino acid aminotransferase [EC:2.6.1.42] |
| 118 | Leucine dehydrogenase [EC:1.4.1.9] |
| 119 | 2-Isopropylmalate synthase [EC:2.3.3.13] |
| 120 | 3-Isopropylmalate dehydratase [EC:4.2.1.33] |
| | **Lysine biosynthesis** |
| 121 | Aspartate kinase [EC:2.7.2.4] |
| 122 | Aspartate-semialdehyde dehydrogenase [EC:1.2.1.11] |

| | |
|---|---|
| 123 | 4-Hydroxy-tetrahydrodipicolinate synthase [EC:4.3.3.7] |
| 124 | 4-Hydroxy-tetrahydrodipicolinate reductase [EC:1.17.1.8] |
| 125 | Tetrahydrodipicolinate N-acetyltransferase [EC:2.3.1.89] |
| 126 | Aminotransferase [EC:2.6.1.-] |
| 127 | Diaminopimelate epimerase [EC:5.1.1.7] |
| 128 | Diaminopimelate decarboxylase [EC:4.1.1.20] |
| | **Terpenoid biosynthetic Pathway** |
| 129 | 1-deoxy-D-xylulose-5-phosphate synthase [EC:2.2.1.7] |
| 130 | 1-deoxy-D-xylulose-5-phosphate reductoisomerase [EC:1.1.1.267] |
| 131 | 2-C-methyl-D-erythritol 4-phosphate cytidylyltransferase [EC:2.7.7.60] |
| 132 | 4-diphosphocytidyl-2-C-methyl-D-erythritol kinase [EC:2.7.1.148] |
| 133 | 2-C-methyl-D-erythritol 2,4-cyclodiphosphate synthase [EC:4.6.1.12] |
| 134 | (E)-4-hydroxy-3-methylbut-2-enyl-diphosphate synthase [EC:1.17.7.11.17.7.3] |
| 135 | (E)-4-hydroxy-3-methylbut-2-enyl-diphosphate synthase [EC:1.17.7.11.17.7.3] |
| 136 | 4-hydroxy-3-methylbut-2-en-1-yl diphosphate reductase [EC:1.17.7.4] |
| 137 | 4-hydroxy-3-methylbut-2-en-1-yl diphosphate reductase [EC:1.17.7.4] |
| 138 | farnesyl diphosphate synthase [EC:2.5.1.1 2.5.1.10] |
| | **Sulfur metabolism** |
| 139 | Sulfate transporter, CysZ-type |
| 140 | Sulfate permease |
| 141 | Sulfur carrier protein FdhD |
| 142 | Homoserine O-succinyltransferase/O-acetyltransferase [EC:2.3.1.462.3.1.31] |
| 143 | Kynurenine---oxoglutarate transaminase / cysteine-S-conjugate beta-lyase / glutamine---phenylpyruvate transaminase [EC:2.6.1.7 4.4.1.13 2.6.1.64] |
| 144 | Cysteine desulfurase (EC 2.8.1.7) |
| 145 | CoA-disulfide reductase (EC 1.8.1.14) / Disulfide bond regulator |
| 146 | Thiosulfate sulfurtransferase, rhodanese (EC 2.8.1.1) |
| | **Heterodisulfide reductase (HDR) system** |
| 147 | Heterodisulfide reductase, cytochrome reductase subunit |
| 148 | heterodisulfide reductase, iron-sulfur binding subunit, putative |
| 149 | Heterodisulfide reductase subunit D-like protein |
| 150 | Heterodisulfide reductase subunit A-like protein |
| 151 | Heterodisulfide reductase subunit C-like protein |
| 152 | Heterodisulfide reductase subunit B-like protein |
| | **Transporter related genes** |
| 153 | Acetate-proton symport |
| 154 | Peptide transporter |
| 155 | Mg/Co/Ni transporter MgtE / CBS domain protein OppF (TC 3.A.1.5.1) |
| 156 | Amino acid ABC transporter, permease protein |
| 157 | Methionine transporter MetT |
| 158 | Ferric iron ABC transporter, iron-binding protein |
| 159 | Oligopeptide transport ATP-binding |
| 160 | Spermidine Putrescine ABC transporter permease component PotB (TC 3.A.1.11.1) |
| 161 | Sodium-dependent phosphate transporter |
| 162 | L-proline glycine betaine binding ABC transporter protein ProX (TC 3.A.1.12.1) / Osmotic adaptation |
| 163 | Maltose/maltodextrin ABC transporter, permease protein MalF |
| 164 | Vitamin $B_{12}$ ABC transporter, B12-binding component BtuF |
| 165 | ABC-type transport system, involved in lipoprotein release, permease component |
| 166 | NADH:ubiquinone oxidoreductase subunit 5 |

167 Putative glutamine transport system permease
168 Ribose ABC transport system, ATP-binding protein RbsA (TC 3.A.1.2.1)
169 Oligopeptide transport ATP-binding protein OppF (TC 3.A.1.5.1)
170 Branched-chain amino acid transport system permease protein LivM (TC 3.A.1.4.1)
171 Na-K-Cl cotransporter
172 Amino acid ABC transporter, ATP-binding protein
173 Glycerol-3-phosphate transporter
174 Ribose ABC transport system, permease protein RbsC (TC 3.A.1.2.1)
175 Spermidine Putrescine ABC transporter permease component potC (TC_3.A.1.11.1)
176 Choline-glycine betaine transporter
177 Maltose/maltodextrin ABC transporter, substrate binding periplasmic protein MalE
178 Magnesium and cobalt transport protein CorA

**ATP Synthesis**

179 F-type H+/Na+-transporting ATPase subunit alpha [EC:7.1.2.2 7.2.2.1]
180 F-type H+/Na+-transporting ATPase subunit beta [EC:7.1.2.2 7.2.2.1]
181 F-type H+-transporting ATPase subunit delta
182 F-type H+-transporting ATPase subunit epsilon
183 F-type H+-transporting ATPase subunit gamma
184 F-type H+-transporting ATPase subunit a
185 F-type H+-transporting ATPase subunit b
186 F-type H+-transporting ATPase subunit c

**Oxygen Detoxification**

187 Superoxide reductase (EC 1.15.1.2)

**$H_2$ production**

[FeFe] hydrogenase (EC 1.12.7.2) 2 operons
Periplasmic [FeFe] hydrogenase large subunit (EC 1.12.7.2) 4 operons

**Amino acid fermentations**

hypothetical protein clustered with lysine fermentation genes
Alanine dehydrogenase (EC 1.4.1.1)
Cystathionine beta-lyase (EC 4.4.1.8)
Tryptophanase (EC 4.1.99.1)

**Membrane Transport**

**ABC transporter oligopeptide (TC 3.A.1.5.1)**

Oligopeptide ABC transporter, periplasmic oligopeptide-binding protein OppA (TC 3.A.1.5.1)
Oligopeptide transport system permease protein OppB (TC 3.A.1.5.1)

**ABC transporter dipeptide (TC 3.A.1.5.2)**

Dipeptide-binding ABC transporter, periplasmic substrate-binding component (TC 3.A.1.5.2)

**Magnesium transport**

Mg(2+) transport ATPase protein C

**Supplementary Table S3:** Average nucleotide identity (ANI) and digital-DDH between strains SD5$^{T}$ (1), BL5 (2) and *Psychrilyobacter atlanticus* JCM 14977$^{T}$ (3).

| **Strains** | **1** | | **2** | | **3** | |
|---|---|---|---|---|---|---|
| | ANI | Digital-DDH | ANI | Digital-DDH | ANI | Digital-DDH |
| **1** | 100 | 100 | 99.9 | 99.9 | 86.6 | 32.9 |
| **2** | 99.9 | 99.9 | 100 | 100 | 86.5 | 32.9 |
| **3** | 86.6 | 32.9 | 86.5 | 32.9 | 100 | 100 |

**Supplementary Table S4: ***Differentiating characteristics between strain SD5$^T$, BL5 and *Psychrilyobacter atlanticus* JCM 14977$^T$.

| **Characteristic** | **SD5$^T$** | **BL5** | *P. atlanticus* JCM 14977$^T$ |
|---|---|---|---|
| Natural Habitat | Marine water | Marine water | Marine sediment |
| Cell shape | Rod to oval | Rod to oval | short rod |
| Cell size (µm) | Rod (0.6-0.7x3-6) oval (diameter, 1.1-1.2) | Rod (0.6-0.7x3-6) Oval (diameter, 1.1-1.2) | 0.5-0.6x0.5-1.0 |
| Growth at 50 MPa | + | + | - |
| Growth at 32 mM of sulfide concentration | + | + | - |
| Optimum (range) pH | 7.0-8.0 (6.5-8.8) | 7.0-8.0 (6.5-8.8) | 7.0-7.5 (6.5-9.0) |
| Optimum (range) NaCl (%) | 2-3 (0.5-5.5) | 2-3 (0.5-5.5) | 1.5-2.5 (0.5-5.5) |
| Optimum (range) temperature (°C) | 23-25 (4-35) | 23-25 (4-35) | 18-20 (4-30) |
| **Hydrolysis of** | | | |
| Cellulose | + | + | - |
| Chitin | + | + | - |
| Starch | + | + | - |
| **Organic substrate utilized for growth** | | | |
| Cellulose | + | + | - |
| Fumarate | - | - | + |
| **API 20A** | | | |
| Urease | + | + | - |
| Gelatin | - | - | + |
| Esculin | - | - | + |
| D-Raffinose | - | + | + |
| G+C (mol %) | 33.8 | 33.8 | 31.9 |

*Data obtained from authors laboratory.

1, *Psychrilyobacter piezotolerans* SD5$^T$; 2, BL5; 3, *Psychrilyobacter atlanticus* JCM 14977$^T$; Both strains are negative for catalase and oxidase activity; Positive for glucose, lactate, glycerol, xylose, galactose, cellobiose, maltose and lactose, aspartate, threonine, glutamate, and lysine fermentation; utilized D-glucose, cellobiose, sucrose, pyruvate, aspartic acid, glutamic acid, L-lysine and acetate; both strains are positive for D-glucose, D-mannitol, D-lactose (bovine origin), D-saccharose (sucrose), D-maltose, salicin, D-xylose, L-arabinose, glycerol, D-cellobiose and D-mannose and negative for D-melezitose,

D-raffinose, D-sorbitol, L-rhamnose, D-trehalose and indole under API A kit test; +, positive/utilized/required; -, negative/not utilized/not required; ND, not determined.

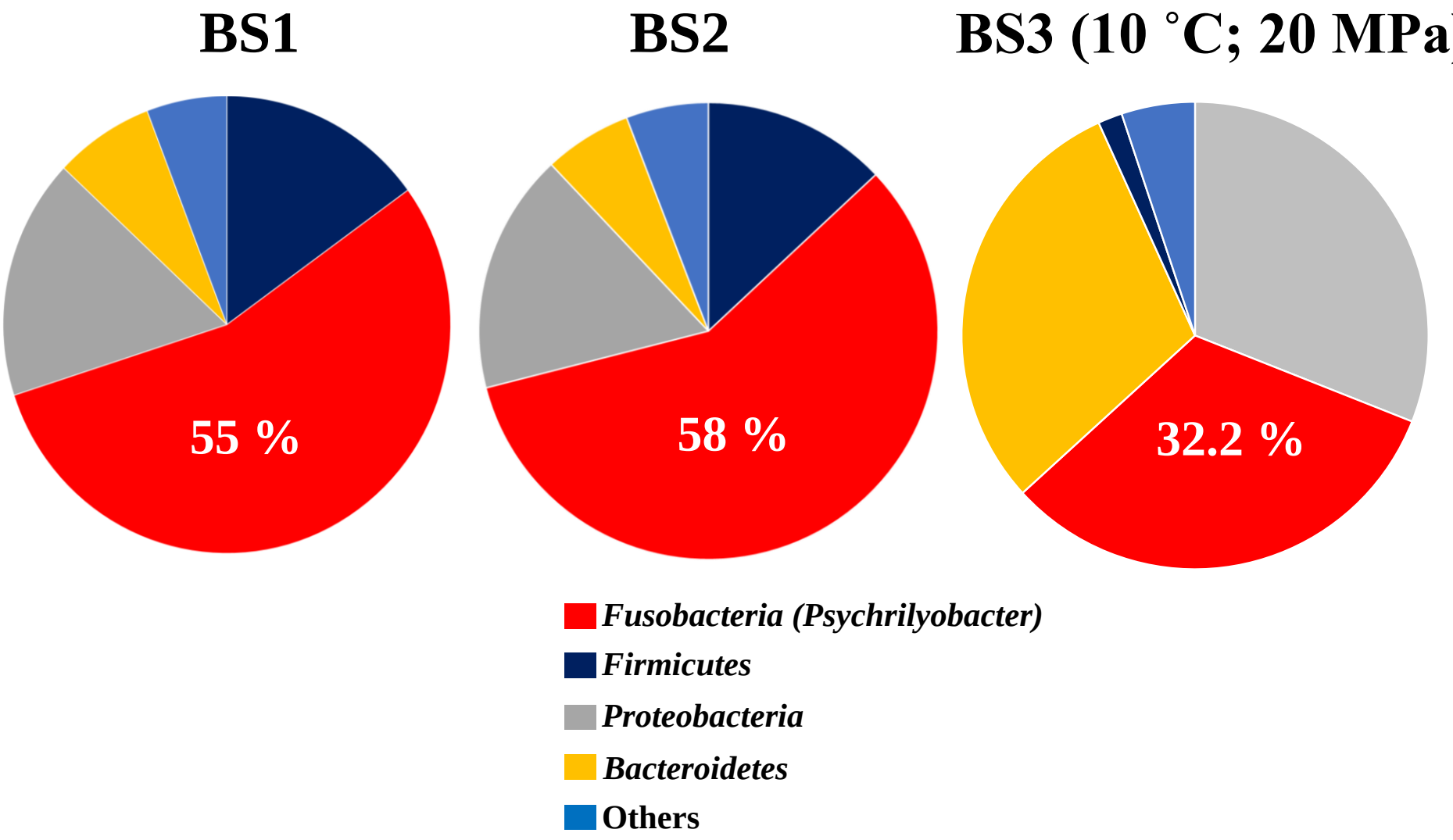


**Supplemental Fig. S1:** Relative abundance (in % of total bacterial and archaeal 16S rRNA gene sequences) of the *Psychrilyobacter* spp. and the composition of the rest of the microbial community in the enrichments using the growth media BS1, BS2 and BS3.

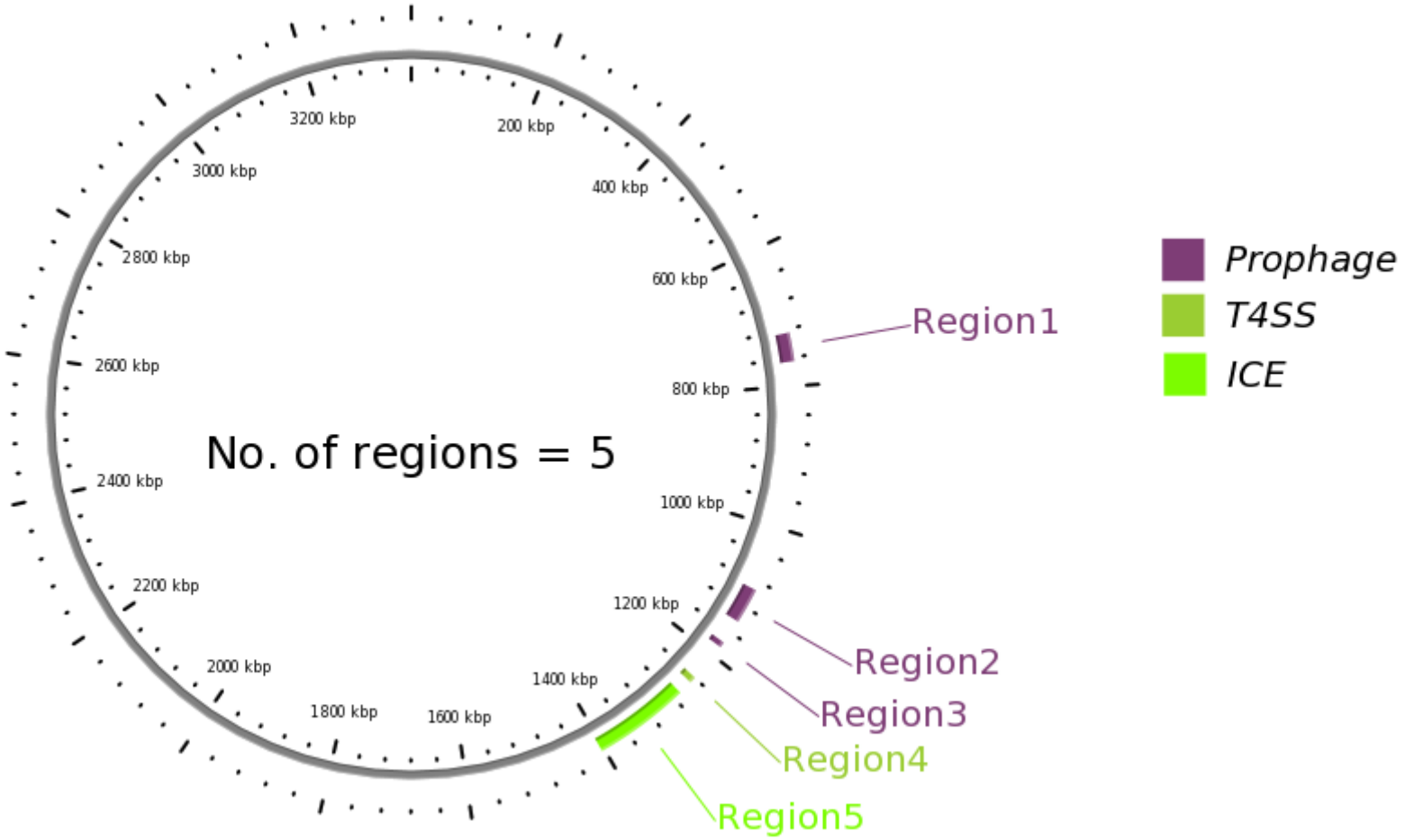


**Supplemental Fig. S2:** Putative virulence related regions identified in the genomes of strains SD5$^{T}$ and BL5.